Fermilab–PUB–89/91–T
BNL-42398

The one particle inclusive differential cross section for heavy quark production in hadronic collisions

P. Nason[1]
Institute of Theoretical Physics,
ETH - Hönggerberg,
CH-8093 Zurich, Switzerland
S. Dawson
Brookhaven National Laboratory,
Upton, New York 11973, USA
R. K. Ellis
Fermi National Accelerator Laboratory
P. O. Box 500, Batavia, Illinois 60510, USA
April 2, 1989

Abstract

We present formulae and results on the one particle inclusive differential cross section for heavy quark production in hadronic collisions, including the $O(\alpha_S^3)$ radiative corrections. We discuss the general range of applicability of the results and present transverse momentum and rapidity distributions. We consider the production of top, bottom and charm quarks at energies of interest for current experiments.

[1]Supported by the Swiss National Foundation

1. Introduction

In this paper we consider the differential distribution for the one particle inclusive production of a heavy quark in hadronic collisions including the $O(\alpha_S^3)$ corrections. This paper is a sequel to ref. [1] in which we discussed the effect of the $O(\alpha_S^3)$ corrections on the total cross section. A limited number of phenomenological results on the differential cross section using the $O(\alpha_S^3)$ calculation have already been presented[2]. For a discussion of the influence of radiative corrections on the photoproduction of heavy quarks we refer the reader to ref. [3].

For a general discussion of the motivation for this work, we refer the reader to ref. [1]. A complete description of the calculation including technical details will be published elsewhere[4]. In this paper, we want to discuss only those aspects of our result which are relevant for the one particle inclusive differential cross section.

The process of one heavy quark inclusive production is depicted in fig. 1. The corresponding QCD formula is

$$\frac{E\, d^3\sigma}{d^3k} = \sum_{i,j} \int dx_A dx_B \left[\frac{E\, d^3\hat{\sigma}_{ij}(x_A P_A, x_B P_B, k, m, \mu)}{d^3k}\right] F_i^A(x_A,\mu)\, F_j^B(x_B,\mu) \tag{1.1}$$

where $F_i^{A,B}$ are the number densities for the i^{th} parton in the incoming hadrons A and B, with momenta P_A and P_B respectively. The parton short distance section is denoted by $\hat{\sigma}$. The mass of the produced heavy quark is m and μ is the subtraction scale for ultraviolet and collinear divergences. Perturbative QCD gives a prescription for calculating $\hat{\sigma}$ as a power series expansion in $\alpha_S(\mu^2)$. The corrections to eq. 1.1 are suppressed by powers of the heavy quark mass.

We have obtained an analytic expression for $Ed^3\hat{\sigma}/d^3k$ up to order α_S^3. The partonic subprocesses which contribute in this order are,

$$\begin{array}{llll} g+g\to Q+X, & q+\overline{q}\to Q+X, & g+q\to Q+X, & g+\overline{q}\to Q+X \\ g+g\to \overline{Q}+X, & \overline{q}+q\to \overline{Q}+X, & g+\overline{q}\to \overline{Q}+X, & g+q\to \overline{Q}+X. \end{array} \tag{1.2}$$

The process $g+g \to Q+X$ has also been calculated in ref. [5]. Note that to this order in perturbation theory the cross section for the production of a quark differs from the cross section for the production of an antiquark. The existence of this effect has been noted elsewhere in the literature[6,7]. This paper gives the first complete treatment including both real and virtual diagrams. The numerical significance of this effect will be discussed later. The analytic expressions for the one particle inclusive differential cross section are too long to be published in a journal. They are available as fortran routines the usage of which is described in Appendix A.

In the first four sections of this work, we examine the structure of the differential cross section in perturbation theory. In Section II, we give our kinematic definitions and illustrate the general structure of the formulae for the leading and next to leading order cross section. We also exhibit the structure of the soft singularity, the subtraction scale dependence and the $1/v$ singularity which is due to the exchange of Coulomb gluons.

To incorporate the radiative corrections consistently in the calculation of a physical cross section, all the component parts of the calculation must be included at next to leading order accuracy. One must use a next to leading order determination of both the coupling constant and the structure functions. All quantities must be consistently defined within the same renormalisation and factorisation scheme. The ambiguities in the inclusion of flavour thresholds in the evolution of the running coupling and the structure functions must be resolved at next to leading order. In view of the large number of subtleties related to the scheme dependence in QCD beyond the leading order, we have dedicated two sections to the discussion of these issues. In Section III we specify our subtraction scheme. In Section IV we give the explicit formula needed to change from one subtraction scheme to another. This is necessary, because the parametrisations of the structure functions presently available are defined in different schemes. The reader who is interested in using the formulae for the radiative corrections, will find all the information needed in sections I to IV.

To assess the reliability of the phenomenological predictions, we must understand the sources of theoretical error. Potential sources of error are the lack of precise knowledge of Λ_{QCD} and of the structure functions and the effect of corrections of yet higher order. Some of these uncertainties are also present in the prediction for the total cross section and have been discussed elsewhere[8]. In the case of the differential distribution, we have a new uncertainty when k_T is much larger than the heavy quark mass, due to the presence of large logarithms of k_T^2/m^2. This problem is discussed in section V.

Phenomenological predictions are given in Section VI. The reader who is only interested in the phenomenological results can turn directly to section VI.

2. The structure of short distance cross section

In fig. 2 we show the diagrams contributing to the lowest order parton differential cross section. The lowest order formulae are given by[9],

$$\begin{aligned}
\frac{d\hat{\sigma}_{gg}}{dyd^2k_T} &= \frac{\alpha_S^2}{s^2} h_{gg}^{(0)}(\tau_1,\rho)\delta(\tau_x) \\
h_{gg}^{(0)}(\tau_1,\rho) &= \frac{2T_f}{D_A}\left(\frac{C_f}{\tau_1\tau_2}-C_A\right)\left(\tau_1^2+\tau_2^2+\rho-\frac{\rho^2}{4\tau_1\tau_2}\right) \qquad (2.1)
\end{aligned}$$

$$\begin{aligned}
\frac{d\hat{\sigma}_{q\bar{q}}}{dyd^2k_T} &= \frac{\alpha_S^2}{s^2} h_{q\bar{q}}^{(0)}(\tau_1,\rho)\delta(\tau_x) \\
h_{q\bar{q}}^{(0)}(\tau_1,\rho) &= \frac{C_f^2}{D_A}\left(2\tau_1^2+2\tau_2^2+\rho\right) \qquad (2.2)
\end{aligned}$$

where C_A and C_f are the Casimir invariants for the adjoint and the fermion representation and D_A is the dimension of the adjoint representation. For the particular case of colour SU(3) we have,

$$C_A = 3,\ C_f = \frac{4}{3},\ T_f = \frac{1}{2},\ D_A = 8. \qquad (2.3)$$

The kinematic variables are defined as,

$$\begin{aligned}
s &= (p_A + p_B)^2 && (2.4) \\
\rho &= \frac{4m^2}{s} && (2.5) \\
\tau_1 &= (k\cdot p_A)/(p_B\cdot p_A) && (2.6) \\
\tau_2 &= (k\cdot p_B)/(p_A\cdot p_B) && (2.7)
\end{aligned}$$

$$\tau_x = \frac{[(p_A + p_B - k)^2 - m^2]}{s} = 1 - \tau_1 - \tau_2. \tag{2.8}$$

where p_A and p_B are the momenta of the incoming partons and k is the momentum of the detected heavy quark. Observe that the lowest order formulae are proportional to $\delta(\tau_x)$, because, according to eq. 2.8, when the recoiling quark is on shell we have $\tau_x = 0$. The virtual corrections to the lowest order processes are therefore also proportional to $\delta(\tau_x)$.

Some examples of graphs that contribute to the gluon gluon initiated process in order α_S^3 are shown in fig. 3. Fig. 3a displays some virtual graphs. Their interference with the lowest order graphs contributes in order α_S^3. The squares of the real graphs shown in fig. 3b also give contributions of order α_S^3. Observe that in the real graphs the variable τ_x is not constrained to be zero. In the limit $\tau_x \to 0$ the light parton in the final state is soft (i.e. it has vanishing energy).

The final result for the partonic cross section has the following form,

$$\frac{d\hat{\sigma}_{ij}}{dy d^2 k_T}(p_A, p_B, k, m, \mu, \alpha_S) =$$

$$H_{ij}^{(0)}(p_A, p_B, k, m, \alpha_S) + H_{ij}^{(1)}(p_A, p_B, k, m, \mu, \alpha_S) + O(\alpha_S^4) \tag{2.9}$$

$$H_{ij}^{(0)}(p_A, p_B, k, m, \alpha_S) = \frac{\alpha_S^2}{s^2} h_{ij}^{(0)}(\tau_1, \rho)\delta(\tau_x) \tag{2.10}$$

$$H_{ij}^{(1)}(p_A, p_B, k, m, \mu, \alpha_S) = \frac{\alpha_S^2}{s^2}\left(\frac{\alpha_S}{2\pi}\right)\Bigg[\left(h_{ij}^{(d)}(\tau_1, \rho) + \xi \overline{h}_{ij}^{(d)}(\tau_1, \rho)\right)\delta(\tau_x)$$

$$+\left(h_{ij}^{(+)}(\tau_1, \tau_2, \rho) + \xi \overline{h}_{ij}^{(+)}(\tau_1, \tau_2, \rho)\right)\left[\frac{1}{\tau_x}\right]_+ + h_{ij}^{(l)}(\tau_1, \tau_2, \rho)\left[\frac{\log(\tau_x)}{\tau_x}\right]_+\Bigg] \tag{2.11}$$

The dependence on the scale μ is contained in the variable ξ.

$$\xi = \ln(\mu^2/m^2) \tag{2.12}$$

The plus distributions are defined in the following way

$$\int_0^1 d\tau_x f(\tau_x)\left[\frac{1}{\tau_x}\right]_+ = \int_0^1 d\tau_x \frac{f(\tau_x) - f(0)}{\tau_x} \tag{2.13}$$

$$\int_0^1 d\tau_x f(\tau_x)\left[\frac{\log(\tau_x)}{\tau_x}\right]_+ = \int_0^1 d\tau_x (f(\tau_x) - f(0))\frac{\ln \tau_x}{\tau_x}. \tag{2.14}$$

The singularities at $\tau_x = 0$ are due to the emission of a real gluon with vanishing energy. The plus prescription which regulates the divergences is a consequence of the cancellation of divergences due to real and virtual soft gluons. The coefficients of $\left[\frac{1}{\tau_x}\right]_+$, ($h^{(+)}$ and $\bar{h}^{(+)}$), could be further divided into terms which vanish as $\tau_x = 0$ and give a regular contribution, plus a remainder which gives a singular contribution. This separation is to a certain extent arbitrary. We have chosen not to perform this separation, since it does not give any practical advantage, and it complicates the notation.

The formulae for $h^{(0)}, h^{(d)}, h^{(+)}, h^{(l)}$ and the corresponding overlined quantities are available as fortran routines. The usage of these routines is described in Appendix A.

The μ dependence of our result is determined by renormalisation group arguments,

$$\frac{\partial H_{ij}^{(1)}(p_A, p_B, k, m, \mu, \alpha_S)}{\partial \ln \mu^2} = 2\alpha_S b_0 H_{ij}^{(0)}(p_A, p_B, k, m, \mu, \alpha_S)$$
$$-\frac{\alpha_S}{2\pi} \sum_k \int_0^1 dz_A H_{kj}^{(0)}(z_A p_A, p_B, k, m, \mu, \alpha_S) P_{ki}(z_A)$$
$$-\frac{\alpha_S}{2\pi} \sum_k \int_0^1 dz_B H_{ik}^{(0)}(p_A, z_B p_B, k, m, \mu, \alpha_S) P_{kj}(z_B) \tag{2.15}$$

where $P_{ij}(z)$ are the Altarelli-Parisi[10] splitting functions

$$\begin{aligned}
P_{gq}(z) &= C_f\left[\frac{1+(1-z)^2}{z}\right] \\
P_{qg}(z) &= T_f\left[z^2+(1-z)^2\right] \\
P_{gg}(z) &= 2C_A\left[\frac{z}{(1-z)_+} + \frac{1-z}{z} + z(1-z)\right] + 2\pi b_0 \delta(1-z) \\
P_{qq}(z) &= C_f\left[\frac{1+z^2}{(1-z)_+} + \frac{3}{2}\delta(1-z)\right]
\end{aligned} \tag{2.16}$$

and

$$\frac{\partial \alpha_S}{\partial \ln \mu^2} = -b_0 \alpha_S^2 + \ldots, \quad b_0 = \frac{11 C_A - 4 T_f n_{\rm lf}}{12\pi} \tag{2.17}$$

where $n_{\rm lf}$ is the number of flavours excluding the heavy one. Using eqs. 2.10 and 2.11 we can evaluate $\overline{h}^{(d)}$ and $\overline{h}^{(+)}$ in terms of the lowest order cross sections and the Altarelli-Parisi functions,

$$\overline{h}_{ij}^{(d)}(\tau_1,\rho)\delta(\tau_x)+\overline{h}_{ij}^{(+)}(\tau_1,\tau_2,\rho)\left[\frac{1}{\tau_x}\right]_+ = 4\pi b_0 h_{ij}^{(0)}(\tau_1,\rho)\delta(\tau_x)$$
$$-\int_0^1 \frac{dz_A}{z_A^2} h_{kj}^{(0)}\left(\tau_1,\frac{\rho}{z_A}\right)\delta\left(1-\tau_1-\frac{\tau_2}{z_A}\right)P_{ki}(z_A)$$
$$-\int_0^1 \frac{dz_B}{z_B^2} h_{ik}^{(0)}\left(\frac{\tau_1}{z_B},\frac{\rho}{z_B}\right)\delta\left(1-\frac{\tau_1}{z_B}-\tau_2\right)P_{kj}(z_B) \tag{2.18}$$

Integrating the delta functions one obtains the formula,

$$\overline{h}_{ij}^{(d)}(\tau_1,\rho)\delta(\tau_x)+\overline{h}_{ij}^{(+)}(\tau_1,\tau_2,\rho)\left[\frac{1}{\tau_x}\right]_+ = 4\pi b_0 h_{ij}^{(0)}(\tau_1,\rho)\delta(\tau_x)$$
$$-\frac{1}{\tau_2}h_{kj}^{(0)}\left(\tau_1,\frac{\rho(1-\tau_1)}{\tau_2}\right)P_{ki}\left(\frac{\tau_2}{1-\tau_1}\right)-\frac{1}{\tau_1}h_{ik}^{(0)}\left(1-\tau_2,\frac{\rho(1-\tau_2)}{\tau_1}\right)P_{kj}\left(\frac{\tau_1}{1-\tau_2}\right) \tag{2.19}$$

we get,

$$\overline{h}_{gg}^{(d)}(\tau_1,\rho)=(2C_A\ln(\tau_1(1-\tau_1)))h_{gg}^{(0)}(\tau_1,\rho) \tag{2.20}$$
$$\overline{h}_{gg}^{(+)}(\tau_1,\tau_2,\rho)=$$
$$-\frac{1}{\tau_2}h_{gg}^{(0)}\left(\tau_1,\frac{\rho(1-\tau_1)}{\tau_2}\right)\tau_x P_{gg}\left(\frac{\tau_2}{1-\tau_1}\right)-\frac{1}{\tau_1}h_{gg}^{(0)}\left(1-\tau_2,\frac{\rho(1-\tau_2)}{\tau_1}\right)\tau_x P_{gg}\left(\frac{\tau_1}{1-\tau_2}\right) \tag{2.21}$$

$$\overline{h}_{q\bar{q}}^{(d)}(\tau_1,\rho)=(4\pi b_0+2C_f\ln(\tau_1(1-\tau_1))-3C_f)h_{q\bar{q}}^{(0)}(\tau_1,\rho) \tag{2.22}$$
$$\overline{h}_{q\bar{q}}^{(+)}(\tau_1,\tau_2,\rho)=$$
$$-\frac{1}{\tau_2}h_{q\bar{q}}^{(0)}\left(\tau_1,\frac{\rho(1-\tau_1)}{\tau_2}\right)\tau_x P_{qq}\left(\frac{\tau_2}{1-\tau_1}\right)-\frac{1}{\tau_1}h_{q\bar{q}}^{(0)}\left(1-\tau_2,\frac{\rho(1-\tau_2)}{\tau_1}\right)\tau_x P_{qq}\left(\frac{\tau_1}{1-\tau_2}\right) \tag{2.23}$$

$$\overline{h}_{gq}^{(d)}(\tau_1,\rho)=0 \tag{2.24}$$
$$\overline{h}_{gq}^{(+)}(\tau_1,\tau_2,\rho)=$$
$$-\frac{1}{\tau_2}h_{qq}^{(0)}\left(\tau_1,\frac{\rho(1-\tau_1)}{\tau_2}\right)\tau_x P_{qg}\left(\frac{\tau_2}{1-\tau_1}\right)-\frac{1}{\tau_1}h_{gg}^{(0)}\left(1-\tau_2,\frac{\rho(1-\tau_2)}{\tau_1}\right)\tau_x P_{gq}\left(\frac{\tau_1}{1-\tau_2}\right) \tag{2.25}$$

where all expressions in the above equations are regular as $\tau_x \to 0$.

The terms $h_{gg}^{(d)}$ and $h_{q\bar{q}}^{(d)}$ contain a $1/v$ singularity coming from the virtual diagrams,

$$v = \sqrt{1-\rho} \tag{2.26}$$

is the velocity of the heavy quarks in the parton CM system, (when $\tau_x = 0$). The coefficient of the $1/v$ terms depends whether the produced $Q\bar{Q}$ pair is in a colour singlet or octet state. We find

$$h_{gg}^{(d)}(\tau_1,\rho) \underset{v\to 0}{\to} \frac{\pi^2}{v} h_{gg}^{(0)}(\tau_1,\rho)\left(C_f - \frac{C_A}{2}\right)\left(1 - \frac{C_A}{2(C_f - C_A\tau_1\tau_2)}\right) \tag{2.27}$$

$$h_{q\bar{q}}^{(d)}(\tau_1,\rho) \underset{v\to 0}{\to} \frac{\pi^2}{v} h_{q\bar{q}}^{(0)}(\tau_1,\rho)\left(C_f - \frac{C_A}{2}\right). \tag{2.28}$$

These singularities are due to the diagrams shown in fig. 4 and are analogous to the singularities in electrodynamics responsible for binding in a nonrelativistic Coulomb system. Detailed features of our results which depend on the presence of the $1/v$ singularity should not be trusted. The hadronic cross section is given by the perturbative heavy quark cross section after smearing over the final state. For a treatment of a similar problem in e^+e^- annihilation we refer the reader to ref. [11].

The convolution integral, eq. 1.1 integrates over the $1/v$ singularity and transforms it into a logarithmic singularity at $k_T = 0$. As we will see in the section on phenomenology, the effect of this singularity is too small to be observed. There is therefore no necessity to introduce a special smearing procedure.

3. Renormalisation and factorisation

When calculating a quantity in next to leading order in QCD, one must make a choice of subtraction scheme for both the ultraviolet and the collinear singularities. The formulae for the parton cross sections depend on the scheme chosen. Predictions for physical quantities are scheme independent. The only effect of a change in the renormalisation and factorisation scheme is to distribute the radiative corrections differently between the parton cross section, the structure functions and α_S. When one changes scheme the values of α_S, $\hat{\sigma}$ and the structure functions are all changed.

In a formula for a physical cross section like eq. 1.1 all these changes compensate each other to the requisite order. The net change is of yet higher order in α_S.

In order to give full meaning to our result, we must therefore specify in which subtraction scheme we are working and what are the appropriate definitions of the structure functions and of the coupling constant that should be used in conjunction with our formulae. In this section we define our subtraction scheme.

We used a renormalisation scheme for the ultraviolet divergences which is an extension of the $\overline{\rm MS}$ scheme[12]. The difference with respect to the usual $\overline{\rm MS}$ scheme[13] can be easily stated for gauge invariant quantity, like a cross section for on-shell scattering, since in this case only the charge renormalisation is important. Instead of the charge renormalisation

$$\alpha_S^{\rm bare} = \mu^{2\epsilon}\alpha_S^{\rm ren}\left(1-\frac{\alpha_S^{\rm ren}}{4\pi}\left(\frac{4}{3}T_{\rm f}n_{\rm f}-\frac{11}{3}C_A\right)\frac{1}{\bar\epsilon}\right)+O(\alpha_S^3) \tag{3.1}$$

$$\frac{1}{\bar\epsilon} = \frac{1}{\epsilon}+\ln 4\pi-\gamma_E \tag{3.2}$$

(where $n_{\rm f}$ is the number of flavours including the heavy quark) we used

$$\alpha_S^{\rm bare}=\mu^{2\epsilon}\alpha_S^{\rm ren}\left(1-\frac{\alpha_S^{\rm ren}}{4\pi}\left(\frac{4}{3}T_{\rm f}n_{\rm lf}-\frac{11}{3}C_A\right)\frac{1}{\bar\epsilon}-\frac{\alpha_S^{\rm ren}}{4\pi}\frac{4}{3}T_{\rm f}\left(\frac{1}{\bar\epsilon}+\ln\frac{\mu^2}{m^2}\right)\right) \tag{3.3}$$

where $n_{\rm lf}=n_{\rm f}-1$ is the number of light flavours. The prescription given in eq. 3.3 is obtained when divergences coming from the first $n_{\rm lf}$ fermions are subtracted in the $\overline{\rm MS}$ scheme, while the divergences coming from the heavy quark loop are subtracted at zero external momenta. In this scheme, in the limit of small momenta the heavy flavour decouples. The β function is defined as

$$\beta=\frac{\partial}{\partial\ln\mu^2}\alpha_S^{\rm ren}\bigg|_{\alpha_S^{\rm bare},\epsilon}=-b_0\alpha_S^2+\ldots \tag{3.4}$$

From eq. 3.3 one gets

$$b_0=\frac{11C_A-4T_{\rm f}n_{\rm lf}}{12\pi} \tag{3.5}$$

Therefore the corresponding coupling constant depends only on the number of the light flavours.

Consistency of physical predictions uniquely determines the relation between $\alpha_S^{(n_{\rm lf})}$ and $\alpha_S^{(n_{\rm lf}+1)}$. We denote the number of flavours considered active by a superscript in brackets. From eqs. 3.1 and 3.3, one can see that the two schemes are equal at $\mu = m$. The appropriate value of α_S for the two schemes must also be the same at $\mu = m$, since otherwise physical cross sections would be different in the two schemes. The relation between the couplings in the two schemes is,

$$\alpha_S^{(n_H+1)}(m) = \alpha_S^{(n_H)}(m) \tag{3.6}$$

This is also the matching condition at flavour thresholds that gives the correct relation between α_S determined with a different number of active flavours in the $\overline{\mathrm{MS}}$ scheme. Collinear singularities are also subtracted in the $\overline{\mathrm{MS}}$ scheme.

In summary the steps performed in the calculation of the short distance cross section are as follows,

1. Calculate the spin averaged (bare) parton cross section $\hat{\sigma}^{\mathrm{bare}}$ in $4-2\epsilon$ dimensions including real and virtual corrections. When performing the spin average, it is important to count the spin degrees of freedom of the gluon as $2-2\epsilon$. The number of spin degrees of freedom for fermions is taken to be 2, even in $4-2\epsilon$ dimensions. This is consistent with the conventional normalisation of the spinor traces $\mathrm{Tr}\{1\} = 4$ in the $\overline{\mathrm{MS}}$ scheme. Other choices of the form $\mathrm{Tr}\{1\} = f(4-2\epsilon)$ with $f(4) = 4$ are possible, but define a different renormalisation scheme. Mass counterterms, defined in such a way that the pole of the heavy fermion propagator is not displaced by the radiative corrections, are included at this stage. Self energy insertions on the external lines (with the appropriate weight 1/2) are also included at this stage, so that $\hat{\sigma}^{\mathrm{bare}}$ is the complete cross section for the production of a heavy quark of mass m in $4-2\epsilon$ dimensions. Such a cross section is finite, because both ultraviolet and infrared singularities are regulated in $4-2\epsilon$ dimensions.

2. Substitute the value of α_S^{bare} (given in eq. 3.3) in $\hat{\sigma}^{\mathrm{bare}}$. At this stage, $1/\bar{\epsilon}$ poles associated with ultraviolet divergences drop out.

3. Factor out the collinear singularities, and obtain the short distance cross section $\hat{\sigma}$ according to the formula

$$\frac{E\, d^3\hat{\sigma}_{ij}^{\mathrm{bare}}}{d^3k}(p_i, p_j, k, \epsilon) = \tag{3.7}$$

$$\sum_{k,l}\int dx_1 dx_2 \left[\frac{E\, d^3\hat{\sigma}_{kl}(x_1p_i,x_2p_j,k,\mu,\epsilon)}{d^3k}\right] f_{ki}(x_1,\alpha_S,\epsilon)\; f_{lj}(x_2,\alpha_S,\epsilon)$$

where in the $\overline{\rm MS}$ scheme,

$$f_{ij}(x,\epsilon)=\delta_{ij}\delta(1-x)+\frac{\alpha_S}{2\pi}\frac{1}{\bar{\epsilon}}P_{ij}(x)+O(\alpha_S^2). \tag{3.8}$$

According to the factorisation theorem[14], the parton cross section $\hat{\sigma}$ implicitly defined by the eq. 3.7 is also free of $1/\bar{\epsilon}$ poles associated with collinear singularities and is therefore finite in the limit $\epsilon \to 0$.

The short distance cross section $\hat{\sigma}$ defined in this way together with structure functions with $n_{\rm lf}$ active flavours, can be inserted in eq. 1.1 to obtain a physical cross section. The heavy flavour does not appear as an active parton in eq. 3.7. In complete analogy with the case of α_S, the structure functions for a different number of light flavours must also match at $\mu = m$[15]. More specifically, if we have $n_{\rm lf}$ light flavours and one massive flavour with mass m, the $\overline{\rm MS}$ structure functions with $n_{\rm f} = n_{\rm lf}+1$ active flavours, $F^{(n_{\rm f})}$, must satisfy the conditions,

$$\begin{aligned} F_j^{(n_{\rm lf}+1)}(x,m^2) &= F_j^{(n_{\rm lf})}(x,m^2) \quad \text{for } j\le n_{\rm lf}, & (3.9)\\ F_{n_{\rm lf}+1}^{(n_{\rm lf}+1)}(x,m^2) &= 0. & (3.10)\end{aligned}$$

It should be emphasized that this is a property of the $\overline{\rm MS}$ subtraction scheme, and it is not necessarily true in other schemes.

We have chosen to present our results in the $\overline{\rm MS}$ scheme with $n_{\rm lf}$ light flavours. The heavy flavour does not therefore contribute to the evolution of the coupling and the structure functions in our scheme. All of the effects of the heavy flavour are therefore contained in the partonic cross section. Although other choices are possible, our choice seems to be the most transparent from a physical point of view. Note that the mass of the produced heavy flavour sets the scale of the hard process. The heavy flavour content of the hadrons at a scale of the order of the heavy flavour mass is explicitly a quantity of order α_S. It is therefore natural to include it into the parton cross section $\hat{\sigma}$. We emphasize that the sum over partons in the incoming hadrons runs only over the light partons. Flavour excitation diagrams are not included. The diagrams which appear to correspond to this process are bona fide higher order corrections in this approach[16].

In practice, the standard parametrisations of the structure functions are usually defined for a number of light flavours which changes at the flavour thresholds. For our purposes we would like to have the number of light flavours fixed at the value appropriate for the problem we are treating (i.e., 5 for top, 4 for bottom, 3 for charm). Fortunately, one can easily prove that, when the structure functions are evaluated at a scale $\mu \approx m$ we have,

$$\begin{aligned} F_j^{(n_{lf}+1)}(x,\mu) &= O(\alpha_S), & j &= n_{lf}+1 \\ F_j^{(n_{lf}+1)}(x,\mu) &= F_j^{(n_{lf})}(x,\mu) + O(\alpha_S^2), & j &\leq n_{lf},\ j \neq g \\ F_j^{(n_{lf}+1)}(x,\mu) &= F_j^{(n_{lf})}(x,\mu)\left[1 - \tfrac{2\alpha_S T_f}{3\pi}\ln\tfrac{\mu^2}{m^2}\right] + O(\alpha_S^2), & j &= g \end{aligned} \tag{3.11}$$

One can therefore use structure functions with the heavy flavour included in the evolution provided the subprocesses with incoming heavy quarks are neglected. The difference is either of a higher order in α_S than we are are working or numerically small.

4. Redefinition of the structure functions.

In this section we describe the modifications to our formulae needed to change the subtraction scheme. Our formulae were derived in the $\overline{\mathrm{MS}}$ subtraction scheme described in the previous section. The use of the $\overline{\mathrm{MS}}$ scheme for charge renormalisation is rather widespread. In addition, the modification to our formula with a different definition of α_S are simply obtained. Therefore, we concentrate on the modifications one needs to introduce in order to use a different factorisation scheme for the structure functions.

At leading level, the definition of the parton distribution functions is scheme independent. This is no longer true at subleading level. The difference between structure functions defined in different schemes is of order α_S. In general, there will be a linear relation between parton densities defined in different subtraction scheme. Denoting by f' the parton densities in the new scheme, we have,

$$f_i'(x) = f_i(x) + \frac{\alpha_S}{2\pi}\int_x^1 K_{ij}\left(\frac{x}{z}\right) f_j(z)\frac{dz}{z} + O(\alpha_S^2)$$

$$f_i(x) \;=\; f_i'(x) - \frac{\alpha_S}{2\pi}\int_x^1 K_{ij}\left(\frac{x}{z}\right) f_j'(z)\frac{dz}{z} + O(\alpha_S^2) \tag{4.1}$$

where the lable j denotes any type of parton.

Quantities of physical interest are independent of the scheme which is used. If we have a generic partonic cross section $\sigma_i(xP_A)$, associated with a hard scattering initiated by a parton type i carrying a fraction x of the momentum P_A of hadron A, we must have,

$$\sum_i \int dx\, f_i(x)\sigma_i(xP_A) = \sum_i \int dx\, f_i'(x)\sigma_i'(xP_A) \tag{4.2}$$

Using the substitution eq. 4.1 we obtain the form of the short distance cross section in the new scheme,

$$\sigma_i'(p) = \sigma_i(p) - \frac{\alpha_S}{2\pi}\sum_j \int_0^1 \sigma_j^{(0)}(xp)K_{ji}(x)dx + \mathrm{NNL} \tag{4.3}$$

where NNL stands for next-to-next-to-leading terms. One can easily generalise eq. 4.3 to the case of a process initiated by two partons

$$\sigma_{ij}'(p_A,p_B) = \sigma_{ij}(p_A,p_B) - \frac{\alpha_S}{2\pi}\sum_k \int_0^1 \sigma_{kj}^{(0)}(xp_A,p_B)K_{ki}(x)dx$$

$$-\frac{\alpha_S}{2\pi}\sum_l \int_0^1 \sigma_{il}^{(0)}(p_A,xp_B)K_{lj}(x)dx + \mathrm{NNL} \tag{4.4}$$

We now return to the specific case of the differential cross section for heavy quark production. From eq. 4.4, eq. 2.1, eq. 2.2 and the definition eq. 2.9 we obtain

$$H'^{(1)}_{ij}(p_A,p_B,k,m,\mu,\alpha_S) = H^{(1)}_{ij}(p_A,p_B,k,m,\mu,\alpha_S)$$

$$-\frac{\alpha_S}{2\pi}\frac{\alpha_S^2}{s^2}\frac{1}{\tau_2}\sum_k K_{ki}(\tau_2/(1-\tau_1))\, h_{kj}^{(0)}\left(\tau_1,\rho(1-\tau_1)/\tau_2\right)$$

$$-\frac{\alpha_S}{2\pi}\frac{\alpha_S^2}{s^2}\frac{1}{\tau_1}\sum_l K_{lj}(\tau_1/(1-\tau_2))\, h_{il}^{(0)}\left(1-\tau_2,\rho(1-\tau_2)/\tau_1\right) \tag{4.5}$$

The transformation functions $K_{ij}(x)$ are in general distributions in x. We will limit our attention to the following form which occurs in cases of practical interest.

$$K_{ij}(x) = K_{ij}^{(d)}\delta(1-x) + K_{ij}^{(+)}(x)\left[\frac{1}{1-x}\right]_+ + K_{ij}^{(l)}(x)\left[\frac{\log(1-x)}{1-x}\right]_+ . \tag{4.6}$$

Using the formulae,

$$\begin{aligned}
\delta(a(1-x)) &= \frac{1}{a}\delta(1-x) \\
\left[\frac{1}{a(1-x)}\right]_+ &= \frac{1}{a}\left(\left[\frac{1}{1-x}\right]_+ + \ln(a)\delta(1-x)\right) \\
\left[\frac{\log(a(1-x))}{a(1-x)}\right]_+ &= \frac{1}{a}\left(\left[\frac{\log(1-x)}{1-x}\right]_+ + \ln(a)\left[\frac{1}{1-x}\right]_+ + \tfrac{1}{2}\ln^2(a)\delta(1-x)\right)
\end{aligned} \tag{4.7}$$

the transformation functions in eqs. 4.5 can be expressed in terms of the distributions $\delta(\tau_x)$, $\left[\frac{1}{\tau_x}\right]_+$, $\left[\frac{\log(\tau_x)}{\tau_x}\right]_+$, according to the equations

$$\begin{aligned}
&K_{ij}(\tau_2/(1-\tau_1)) = \\
&(1-\tau_1)\Big\{ \left(K_{ij}^{(d)} - \ln(1-\tau_1)K_{ij}^{(+)}(1) + \tfrac{1}{2}\ln^2(1-\tau_1)K_{ij}^{(l)}(1)\right)\delta(\tau_x) \\
&+ \left(K_{ij}^{(+)}(\tau_2/(1-\tau_1)) - \ln(1-\tau_1)K_{ij}^{(l)}(\tau_2/(1-\tau_1))\right)\left[\frac{1}{\tau_x}\right]_+ \\
&+K_{ij}^{(l)}(\tau_2/(1-\tau_1))\left[\frac{\log(\tau_x)}{\tau_x}\right]_+ \Big\}
\end{aligned} \tag{4.8}$$

$$\begin{aligned}
&K_{ij}(\tau_1/(1-\tau_2)) = \\
&(1-\tau_2)\Big\{ \left(K_{ij}^{(d)} - \ln(1-\tau_2)K_{ij}^{(+)}(1) + \tfrac{1}{2}\ln^2(1-\tau_2)K_{ij}^{(l)}(1)\right)\delta(\tau_x) \\
&+ \left(K_{ij}^{(+)}(\tau_1/(1-\tau_2)) - \ln(1-\tau_2)K_{ij}^{(l)}(\tau_1/(1-\tau_2))\right)\left[\frac{1}{\tau_x}\right]_+ \\
&+K_{ij}^{(l)}(\tau_1/(1-\tau_2))\left[\frac{\log(\tau_x)}{\tau_x}\right]_+ \Big\}
\end{aligned} \tag{4.9}$$

We then obtain

$$\begin{aligned}
&h'^{(d)}_{gg}(\tau_1,\rho) = h^{(d)}_{gg}(\tau_1,\rho) \\
&- \left(K_{gg}^{(d)} - \ln(1-\tau_1)K_{gg}^{(+)}(1) + \tfrac{1}{2}\ln^2(1-\tau_1)K_{gg}^{(l)}(1)\right)h^{(0)}_{gg}(\tau_1,\rho) \\
&- \left(K_{gg}^{(d)} - \ln(1-\tau_2)K_{gg}^{(+)}(1) + \tfrac{1}{2}\ln^2(1-\tau_2)K_{gg}^{(l)}(1)\right)h^{(0)}_{gg}(\tau_1,\rho)
\end{aligned} \tag{4.10}$$

$$h'^{(d)}_{q\bar{q}}(\tau_1,\rho) = h^{(d)}_{q\bar{q}}(\tau_1,\rho)$$
$$-\left(K^{(d)}_{qq} - \ln(1-\tau_1)K^{(+)}_{qq}(1) + \tfrac{1}{2}\ln^2(1-\tau_1)K^{(l)}_{qq}(1)\right)h^{(0)}_{q\bar{q}}(\tau_1,\rho)$$
$$-\left(K^{(d)}_{\bar{q}\bar{q}} - \ln(1-\tau_2)K^{(+)}_{\bar{q}\bar{q}}(1) + \tfrac{1}{2}\ln^2(1-\tau_2)K^{(l)}_{\bar{q}\bar{q}}(1)\right)h^{(0)}_{q\bar{q}}(\tau_1,\rho) \tag{4.11}$$

$$h'^{(d)}_{qg}(\tau_1,\rho) =$$
$$-\left(K^{(d)}_{gq} - \ln(1-\tau_1)K^{(+)}_{gq}(1) + \tfrac{1}{2}\ln^2(1-\tau_1)K^{(l)}_{gq}(1)\right)h^{(0)}_{gg}(\tau_1,\rho)$$
$$-\left(K^{(d)}_{\bar{q}g} - \ln(1-\tau_2)K^{(+)}_{\bar{q}g}(1) + \tfrac{1}{2}\ln^2(1-\tau_2)K^{(l)}_{\bar{q}g}(1)\right)h^{(0)}_{q\bar{q}}(\tau_1,\rho) \tag{4.12}$$

$$h'^{(+)}_{gg}(\tau_1,\tau_2,\rho) = h^{(+)}_{gg}(\tau_1,\tau_2,\rho) -$$
$$\frac{1-\tau_1}{\tau_2}\left(K^{(+)}_{gg}(\tau_2/(1-\tau_1)) - \ln(1-\tau_1)K^{(l)}_{gg}(\tau_2/(1-\tau_1))\right)h^{(0)}_{gg}\left(\tau_1,\rho(1-\tau_1)/\tau_2\right)$$
$$-\frac{1-\tau_2}{\tau_1}\left(K^{(+)}_{gg}(\tau_1/(1-\tau_2)) - \ln(1-\tau_2)K^{(l)}_{gg}(\tau_1/(1-\tau_2))\right)h^{(0)}_{gg}\left(1-\tau_2,\rho(1-\tau_2)/\tau_1\right) \tag{4.13}$$

$$h'^{(+)}_{q\bar{q}}(\tau_1,\tau_2,\rho) = h^{(+)}_{q\bar{q}}(\tau_1,\tau_2,\rho)$$
$$-\frac{1-\tau_1}{\tau_2}\left(K^{(+)}_{qq}(\tau_2/(1-\tau_1)) - \ln(1-\tau_1)K^{(l)}_{qq}(\tau_2/(1-\tau_1))\right)h^{(0)}_{q\bar{q}}\left(\tau_1,\rho(1-\tau_1)/\tau_2\right)$$
$$-\frac{1-\tau_2}{\tau_1}\left(K^{(+)}_{\bar{q}\bar{q}}(\tau_1/(1-\tau_2)) - \ln(1-\tau_2)K^{(l)}_{\bar{q}\bar{q}}(\tau_1/(1-\tau_2))\right)h^{(0)}_{q\bar{q}}\left(1-\tau_2,\rho(1-\tau_2)/\tau_1\right) \tag{4.14}$$

$$h'^{(+)}_{qg}(\tau_1,\tau_2,\rho) = h^{(+)}_{qg}(\tau_1,\tau_2,\rho)$$
$$-\frac{1-\tau_1}{\tau_2}\left(K^{(+)}_{gq}(\tau_2/(1-\tau_1)) - \ln(1-\tau_1)K^{(l)}_{gq}(\tau_2/(1-\tau_1))\right)h^{(0)}_{gg}\left(\tau_1,\rho(1-\tau_1)/\tau_2\right)$$
$$-\frac{1-\tau_2}{\tau_1}\left(K^{(+)}_{\bar{q}g}(\tau_1/(1-\tau_2)) - \ln(1-\tau_2)K^{(l)}_{\bar{q}g}(\tau_1/(1-\tau_2))\right)h^{(0)}_{q\bar{q}}\left(1-\tau_2,\rho(1-\tau_2)/\tau_1\right) \tag{4.15}$$

$$h'^{(l)}_{gg}(\tau_1,\tau_2,\rho) = h^{(l)}_{gg}(\tau_1,\tau_2,\rho) - \frac{1-\tau_1}{\tau_2}K^{(l)}_{gg}(\tau_2/(1-\tau_1))h^{(0)}_{gg}\left(\tau_1,\rho(1-\tau_1)/\tau_2\right)$$

$$-\frac{1-\tau_2}{\tau_1}K_{gg}^{(l)}(\tau_1/(1-\tau_2))h_{gg}^{(0)}(1-\tau_2,\rho(1-\tau_2)/\tau_1) \tag{4.16}$$

$$h'^{(l)}_{q\bar{q}}(\tau_1,\tau_2,\rho)=h^{(+)}_{q\bar{q}}(\tau_1,\tau_2,\rho)-\frac{1-\tau_1}{\tau_2}K_{qq}^{(l)}(\tau_2/(1-\tau_1))h_{q\bar{q}}^{(0)}(\tau_1,\rho(1-\tau_1)/\tau_2)$$

$$-\frac{1-\tau_2}{\tau_1}K_{\bar{q}\bar{q}}^{(l)}(\tau_1/(1-\tau_2))h_{q\bar{q}}^{(0)}(1-\tau_2,\rho(1-\tau_2)/\tau_1) \tag{4.17}$$

$$h'^{(l)}_{qg}(\tau_1,\tau_2,\rho)=h^{(+)}_{qg}(\tau_1,\tau_2,\rho)-\frac{1-\tau_1}{\tau_2}K_{qq}^{(l)}(\tau_2/(1-\tau_1))h_{gg}^{(0)}(\tau_1,\rho(1-\tau_1)/\tau_2)$$

$$-\frac{1-\tau_2}{\tau_1}K_{\bar{q}g}^{(l)}(\tau_1/(1-\tau_2))h_{q\bar{q}}^{(0)}(1-\tau_2,\rho(1-\tau_2)/\tau_1)\,. \tag{4.18}$$

We will be particularly interested in the definition of the structure functions beyond the leading order as given in ref. [17,18]. The relevant transformation functions are

$$K_{qq}(x)=\frac{4}{3}\left\{(1+x^2)\left[\frac{\log(1-x)}{1-x}\right]_+-\frac{3}{2}\left[\frac{1}{1-x}\right]_+-(1+x^2)\frac{\ln(x)}{1-x}\right.$$

$$\left.+3+2x-\left(\frac{9}{2}+\frac{\pi^2}{3}\right)\delta(1-x)\right\} \tag{4.19}$$

$$K_{qg}(x)=\frac{1}{2}\left\{\left(x^2+(1-x)^2\right)\ln\left(\frac{1-x}{x}\right)+8x(1-x)-1\right\} \tag{4.20}$$

$$K_{gq}(x)=-K_{qq}(x) \tag{4.21}$$

$$K_{gg}(x)=-2n_{lf}K_{qg}(x). \tag{4.22}$$

where the transformation functions of the quark densities are defined in such a way that the deep inelastic scattering structure function F_2 is free from radiative corrections in $O(\alpha_S)$. The transformation of the gluon density is instead rather arbitrary, and its only purpose is to preserve the momentum sum rule to order α_S. The decomposition of eqs. 4.19 according to eq. 4.6 gives

$$K_{qq}^{(d)}=-\frac{4}{3}\left(\frac{9}{2}+\frac{\pi^2}{3}\right) \tag{4.23}$$

$$K_{qq}^{(+)}(x)=\frac{4}{3}\left(-\frac{3}{2}-(1+x^2)\ln(x)+(1-x)(3+2x)\right) \tag{4.24}$$

$$K_{qq}^{(l)}(x)=\frac{4}{3}(1+x^2) \tag{4.25}$$

$$K^{(d)}_{qg} = 0 \tag{4.26}$$

$$K^{(+)}_{qg} = \frac{(1-x)}{2}\Big(-(x^2+(1-x)^2)\ln(x) + 8x(1-x) - 1\Big) \tag{4.27}$$

$$K^{(l)}_{qg} = \frac{(1-x)}{2}(x^2+(1-x)^2) \tag{4.28}$$

and $K_{\bar{q}\bar{q}} = K_{qq}$ etc. The transformation functions (4.19) are the appropriate ones to be used in conjunction with the structure functions of ref. [22].

5. Massless limit of the differential cross section

The production of a heavy quark with a transverse momentum much larger than its mass deserves special attention. We therefore consider a hadroproduction experiment performed at fixed k_{T} and S in the limit in which the mass of the heavy quark tends to zero. In this limit we encounter mass singularities, i.e. in the specific case of our calculation terms of the order $\alpha_S^3 \ln(k_{\mathrm{T}}/m)$. We are interested in the zero mass limit for the insight it gives into the structure of these logarithmic terms. In practical experimental configurations in which k_{T} is much larger than m they may give large corrections. In this section we shall discuss this limit, restricting our attention to the example of the $gg \to Q + X$ subprocess.

We consider the zero mass limit of our formulae when the mass of the quark is scaled to zero, $\rho \to 0$ at fixed s and μ. In this limit, we expect terms which are enhanced by a factor of $\ln(\rho)$. Singular terms of this sort originate from configurations that become collinear divergent as we let m go to zero. These configurations are all represented in fig. 5. We will call them flavour excitation, gluon splitting and radiation from the detected quark. Following the usual Altarelli-Parisi scheme, we can immediately write down the singular terms arising from the various contributions illustrated in fig. 5. We get,

$$\lim_{m\to 0} \frac{d\hat{\sigma}_{gg\to Q+X}}{dyd^2k_{\mathrm{T}}}(p_A, p_B, k, m, \mu, \alpha_S) =$$

$$-\frac{\alpha_S}{2\pi}\ln(\rho)\Bigg[\int dz \frac{d\hat{\sigma}_{qg\to q+X}}{dyd^2k_{\mathrm{T}}}(zp_A, p_B, k)P_{qg}(z) + \int dz \frac{d\hat{\sigma}_{gq\to q+X}}{dyd^2k_{\mathrm{T}}}(p_A, zp_B, k)P_{qg}(z)$$

$$+ \int \frac{dz}{z^2} P_{qg}(z) \frac{d\sigma_{gg\to g+X}}{dyd^2(k_{\mathrm{T}}/z)}(p_A, p_B, k/z)$$

$$+\int\frac{dz}{z^2}P_{qq}(z)\frac{d\sigma_{gg\to q+X}}{dyd^2(k_{\rm T}/z)}(p_A,p_B,k/z)\Bigg]+O(\alpha_S) \tag{5.1}$$

where the notation $O(\alpha_S)$ indicates terms that are not enhanced by the logarithmic factor $\ln(\rho)$. The terms in eq. 5.1 are associated respectively with the two flavour excitation graphs, the gluon splitting graph and the contribution of the radiation from the detected quark. The inclusive cross sections appearing in eq. 5.1 are the cross sections for the production of a massless parton of momentum l by the scattering of two massless partons of momenta q_A and q_B[19].

$$\begin{aligned}
\frac{d\sigma_{gg\to g+X}}{dyd^2l_{\rm T}}(q_A,q_B,l) &= \frac{\alpha_S^2}{\hat s}\delta(\hat s+\hat t+\hat u)\frac{4C_A^2}{D_A}\left[3-\frac{\hat t\hat u}{\hat s^2}-\frac{\hat t\hat s}{\hat u^2}-\frac{\hat s\hat u}{\hat t^2}\right]\\
\frac{d\sigma_{gg\to q+X}}{dyd^2l_{\rm T}}(q_A,q_B,l) &= \frac{\alpha_S^2}{\hat s}\delta(\hat s+\hat t+\hat u)\frac{2T_f}{D_A}\left[\frac{C_f}{\hat u\hat t}-\frac{C_A}{\hat s^2}\right](\hat t^2+\hat u^2)\\
\frac{d\sigma_{gq\to q+X}}{dyd^2l_{\rm T}}(q_A,q_B,l) &= \frac{\alpha_S^2}{\hat s}\delta(\hat s+\hat t+\hat u)\frac{2C_f}{D_A}\left[\frac{C_A}{\hat u^2}-\frac{C_f}{\hat s\hat t}\right](\hat s^2+\hat t^2)
\end{aligned} \tag{5.2}$$

where $\hat s=(q_A+q_B)^2, \hat t=(q_A-l)^2, \hat u=(q_B-l)^2$. Using eqs. 5.1 and 5.2 the structure of the logarithms of ρ predicted using the Altarelli-Parisi arguments is,

$$\begin{aligned}
&\lim_{m\to 0}\frac{d\hat\sigma_{gg}}{dyd^2k_{\rm T}}(p_A,p_B,k,m,\mu,\alpha_S) = -\frac{\alpha_S^2}{s^2}\frac{\alpha_S}{2\pi}\ln(\rho)\\
&\Bigg[\frac{4C_A^2}{D_A}\frac{1}{\tau_1+\tau_2}\left(3-\frac{\tau_1\tau_2}{(\tau_1+\tau_2)^2}+\frac{\tau_1}{\tau_2^2}+\frac{\tau_2}{\tau_1^2}\right)T_f\left((\tau_1+\tau_2)^2+\tau_x^2\right)\\
&+\frac{2T_f}{D_A}\left(\frac{\tau_1^2+\tau_2^2}{(\tau_1+\tau_2)^2}\right)\left(C_f\frac{(\tau_1+\tau_2)^2}{\tau_1\tau_2}-C_A\right)C_f\left(\left(1+(\tau_1+\tau_2)^2\right)\left[\frac{1}{\tau_x}\right]_+ +\frac{3}{2}\delta(\tau_x)\right)\\
&+\frac{1}{\tau_2}T_f\left(\frac{\tau_2^2+\tau_x^2}{(1-\tau_1)^2}\right)\frac{2C_f}{D_A}\left(1+(1-\tau_1)^2\right)\left(\frac{C_A}{\tau_1^2}+C_f\frac{1}{1-\tau_1}\right)\\
&+\frac{1}{\tau_1}T_f\left(\frac{\tau_1^2+\tau_x^2}{(1-\tau_2)^2}\right)\frac{2C_f}{D_A}\left(1+(1-\tau_2)^2\right)\left(\frac{C_A}{\tau_2^2}+C_f\frac{1}{1-\tau_2}\right)\Bigg]
\end{aligned} \tag{5.3}$$

Observe the presence of a term proportional to $\delta(\tau_x)$ and a term with the singularity $\left[\frac{1}{\tau_x}\right]_+$, due to the soft radiation from the detected quark.

From our result we find the following limits,

$$\lim_{m\to 0}\overline{h}_{gg}^{(d)}(\tau_1,\rho)=0 \tag{5.4}$$

$$\lim_{m\to 0} \overline{h}^{(+)}_{gg}(\tau_1,\rho) = 0 \tag{5.5}$$

$$\lim_{m\to 0} h^{(d)}_{gg}(\tau_1,\tau_2,\rho) = C_f(\ln^2(\rho) - \ln(\rho))h^{(0)}_{gg}(\tau_1,\rho) \tag{5.6}$$

$$\begin{aligned}
\lim_{m\to 0} \left[\frac{1}{\tau_x}\right]_+ h^{(+)}_{gg}(\tau_1,\tau_2,\rho) &= -C_f(\ln^2(\rho) + \ln(\rho)/2)h^{(0)}_{gg}(\tau_1,\rho)\delta(\tau_x) \\
&- \ln(\rho)\left[\frac{4C_A^2}{D_A}\frac{1}{\tau_1+\tau_2}\left(3 - \frac{\tau_1\tau_2}{(\tau_1+\tau_2)^2} + \frac{\tau_1}{\tau_2^2} + \frac{\tau_2}{\tau_1^2}\right)T_f\left((\tau_1+\tau_2)^2 + \tau_x^2\right)\right. \\
&+\frac{2T_f}{D_A}\left(\frac{\tau_1^2+\tau_2^2}{(\tau_1+\tau_2)^2}\right)\left(C_f\frac{(\tau_1+\tau_2)^2}{\tau_1\tau_2} - C_A\right)C_f(1+(\tau_1+\tau_2)^2)\left[\frac{1}{\tau_x}\right]_+ \\
&+\frac{1}{\tau_2}T_f\left(\frac{\tau_2^2+\tau_x^2}{(1-\tau_1)^2}\right)\frac{2C_f}{D_A}\left(1+(1-\tau_1)^2\right)\left(\frac{C_A}{\tau_1^2} + C_f\frac{1}{1-\tau_1}\right) \\
&\left.+\frac{1}{\tau_1}T_f\left(\frac{\tau_1^2+\tau_x^2}{(1-\tau_2)^2}\right)\frac{2C_f}{D_A}\left(1+(1-\tau_2)^2\right)\left(\frac{C_A}{\tau_2^2} + C_f\frac{1}{1-\tau_2}\right)\right]
\end{aligned} \tag{5.7}$$

where the limit should be understood in a distribution sense because new singularities arise. For example, we made use of the following limit,

$$\frac{1}{\tau_x}\ln\left(1+\frac{4\tau_x}{\rho}\right) \underset{\rho\to 0}{\rightarrow} \left[\frac{\log(\tau_x)}{\tau_x}\right]_+ + \left[\frac{1}{\tau_x}\right]_+ \ln\left(\frac{4}{\rho}\right) - \frac{1}{2}\ln^2\left(\frac{4}{\rho}\right)\delta(\tau_x) \tag{5.8}$$

where the coefficient of the delta function is determined by integration. By combining appropriately eqs. 5.6 and 5.7 one recovers eq. 5.3. This is a valuable check of our calculation.

If we try to compute the differential cross section for the production of a heavy quark with transverse momentum much higher than its mass, the logarithmic terms described in this section become large. At some point, one has $\alpha_S \ln(\rho) \approx 1$, and therefore one must sum all terms of the form $\alpha_S^2(\alpha_S \ln(\rho))^n$ in order to get a sensible leading order result. If one wants to get a correct next to leading order result, one must also include all terms of the form $\alpha_S^3(\alpha_S \ln(\rho))^n$. This can indeed be done. It requires the knowledge of the one particle inclusive cross section for light partons in next to leading order[20], the fragmentation function for any light parton into a heavy quark, and the structure functions for finding a heavy quark in a hadron. Our formula, however, does not provide for this resummation. When trying to predict heavy quark distributions at high k_T using our result, one must therefore be aware of this further theoretical uncertainty.

6. Phenomenological applications.

In this section we examine the effect of the radiative corrections on the differential distribution for the inclusive production of one heavy quark. We cannot describe our results for all energies and processes, but we will try to give an overview of the impact of our results for present and future experiments.

There are various sources of uncertainty one has to examine before making phenomenological predictions. Firstly, there are uncertainties due to our poor knowledge of the structure functions and of the coupling constant α_S. These uncertainties will be treated in a way similar to ref. [8]. We use three different sets of structure functions (DFLM) from Diemoz *et al.*[22], obtained by fitting the same data set with three different values of $\Lambda_4 = 160,\ 260,\ 360$ MeV, ($\Lambda_5 = 101,\ 173,\ 250$ MeV). The values of Λ in the $\overline{\mathrm{MS}}$ scheme with four or five flavours of effectively massless quarks are denoted by Λ_4 and Λ_5 respectively. The DFLM structure functions reflect the uncertainty in the deep inelastic data, the error in the knowledge of α_S and the correlation between the determination of the gluon distribution function and Λ. We will also present some results obtained using the MRS structure functions of Martin *et al.*[23].

Uncalculated effects of even higher order are an another important source of uncertainty. A reasonable way to estimate these effects is by variation of the factorisation and renormalisation scale μ. If the whole perturbation expansion for the cross section were known, it would be formally independent of the value chosen for μ. The residual μ dependence, present in perturbation theory at any finite order, is compensated in the complete perturbation series by the higher order terms. The residual μ dependence can thus be considered an estimate of the magnitude of higher order effects. The scale μ should be chosen to be of the same order as the large scale Q, which characterises the hard process under consideration. This choice avoids the appearance of large logarithms of the form $\ln(Q/\mu)$ in the perturbation series. In the differential cross section for heavy quark production we have two mass scales, m or k_{T}. We will chose $\mu = \mu_0 \equiv \sqrt{(k_{\mathrm{T}}^2 + m^2)}$ as our central value. The scale choices $\mu = 2\mu_0$ and $\mu = \mu_0/2$ will be used to test the sensitivity of the result to variations in μ. When $k_{\mathrm{T}} \approx m$, this choice avoids the appearance of large logarithmic terms. When $k_{\mathrm{T}} \gg m$ the appearance of logarithmic terms cannot be avoided because of the presence of two widely different scales. If we maintain the choice $\mu \approx \sqrt{(k_T^2 + m^2)}$, the structure of these logarithmic terms is well known. It has been analysed in detail in sec. V. We will therefore be able to give an estimate of the size of the logarithmic terms which appear in the order α_S^4.

A further source of uncertainty is due to the poor knowledge of the mass of the heavy quark. Because of the steeply falling parton luminosities changes in mass of the heavy quark can lead to significant changes in the cross-section particularly at low energy. This effect will be examined from case to case.

Unless stated otherwise, the differential cross sections we present are the average of the quark and antiquark production cross sections. The difference between the quark and antiquark production cross sections is small in all cases we have examined. The differential distribution in k_T will be always given as $d\sigma/dk_T^2 \equiv \pi d^2\sigma/d^2k_T$.

6.1. Collider Energies

We begin by considering top production at collider energies. In fig. 6 we show the various contributions to the inclusive differential cross section for the production of a 40 GeV top quark at $\sqrt{S} = 630$ GeV and $y = 0$. We have used our central values of the parameters, $\Lambda_5 = 173$ MeV and $\mu = \sqrt{(k_T^2 + m^2)}$. At this energy the gluon-quark subprocess is negligible and the gg fusion and $q\overline{q}$ annihilation mechanisms give about the same contribution. The rise in the gg contribution and the dip in $q\overline{q}$ contribution, evident at low k_T, are effects of the $1/v$ singularity. This was discussed in Sec. II. At this energy the two effects tend to cancel in the total. As explained in ref. [1] we expect a depletion of the cross section if the $q\overline{q}$ mechanism dominates and an enhancement if the gg mechanism prevails.

In figs. 7, 8, 9 and 10 we present the differential cross sections for top production at CERN and FNAL energies. The top quark mass has been taken to be 40 or 80 GeV. We also show the corresponding lowest order results, evaluated with the same value of the parameters. The lowest order results have been multiplied by an arbitrary factor which varies from case to case so that one can compare the shapes of the two curves directly. These graphs demonstrate that, with the same choice of the parameters, the shape of the differential distribution in $O(\alpha_S^3)$ is the same as in $O(\alpha_S^2)$. We conclude that the shape of the differential distribution for the production of a top quark is unlikely to be modified by higher order corrections in kinematic regions in which the cross section is large. In tables 1, 2, 3, and 4, we also give the differential cross section at typical values of k_T and y, together with the variations in the cross section when Λ_5 is changed from its central value of 173 MeV to 101 or 250 MeV and when μ is changed from its central value $\mu_0 = \sqrt{(k_T^2 + m_t^2)}$ to $2\mu_0$ or $\mu_0/2$. The sum in quadrature of the positive (negative) variations is also given. The errors on the top cross section are moderate.

We now turn our attention to bottom production at colliders. We remind the reader that the uncertainties in the prediction of the total bottom cross section at collider energies are large[1,8]. Nevertheless the shape of the $O(\alpha_S^3)$ differential distribution is remarkably similar to the lowest order shape. This is illustrated in figs. 11 and 12 where we plot the $O(\alpha_s^3)$ differential cross section, together with the lowest order contribution scaled by an arbitrary factor.

There is a new uncertainty in the differential cross section when $k_T \gg m$, due to the presence of large logarithms of k_T/m. For top production, this uncertainty is irrelevant at present energies since the production rate is negligible at $k_T \gg m_t$. For the production of bottom and charm the large k_T region is of great experimental importance, so we will try to estimate the effect of the large logarithms. If we choose $\mu \approx \sqrt{(k_T^2 + m^2)}$, the structure of the logarithmic terms is as explained in Sec. V. The sensitivity to the choice of μ can be considered as a first estimate of the error induced by the presence of the logarithmic terms. To obtain a more reliable estimate of their effect we have calculated a limited number of terms of the order $\alpha_S^2(\alpha_S \ln(k_T/m))^2$. The estimate is performed by iteration of the Altarelli-Parisi equation. The resultant corrections can be ascribed to the diagrams shown in in fig. 13. Their contribution is not very large in the observed k_T range and always tends to soften the k_T spectrum. We have not used this estimate to change our central prediction, but instead have included it as a further source of uncertainty. It should be pointed out that this is an incomplete treatment of the logarithmic terms. In fact, it is possible to sum all terms of the form $\alpha_S^2(\alpha_S \ln(k_T/m))^n$ and $\alpha_S^3(\alpha_S \ln(k_T/m))^n$. This calculation has not yet been performed.

Values of the differential cross section for bottom production are given in tables 5 and 6, for some typical values of the rapidity and transverse momentum. Our estimates of the theoretical uncertainties are also shown.

It is interesting to compare our results with the UA1[24] data for the production of bottom. The values quoted by the UA1 collaboration are as follows.

$$\begin{aligned}
\sigma(p\bar{p} \to b + X,\ k_T > 6.0\ GeV,\ |y| < 1.5) &= 2.25 \pm 1.62\ \mu\mathrm{b} \\
\sigma(p\bar{p} \to b + X,\ k_T > 6.5\ GeV,\ |y| < 1.5) &= 1.2 \pm .66\ \mu\mathrm{b} \\
\sigma(p\bar{p} \to b + X,\ k_T > 10\ GeV,\ |y| < 1.5) &= .415 \pm .199\ \mu\mathrm{b} \\
\sigma(p\bar{p} \to b + X,\ k_T > 15\ GeV,\ |y| < 1.5) &= .21 \pm .0945\ \mu\mathrm{b} \\
\sigma(p\bar{p} \to b + X,\ k_T > 23\ GeV,\ |y| < 1.5) &= .038 \pm .0175\ \mu\mathrm{b} \\
\sigma(p\bar{p} \to b + X,\ k_T > 32\ GeV,\ |y| < 1.5) &= .0115 \pm .00552\ \mu\mathrm{b}. \qquad (6.1)
\end{aligned}$$

The sum of the cross section for the production of a b and the cross section for the production of a $\bar{b}$ quark is given by twice the above numbers. In fig. 14 we show our central prediction, together with an error band. In table 7, we give our prediction of the cross section, together with our estimate of the relevant theoretical uncertainties. The agreement is remarkably good at relatively low k_T, but at high k_T the data lies above the theoretical result. Due to the large uncertainties in both the theoretical prediction and the data, we do not yet consider this discrepancy of great importance. We have obtained similar results by using the structure functions of ref. [23]. At $k_{min} = 32$ GeV using the scale choice $\mu = \mu_0$ we get,

$$\begin{aligned}
\text{MRS set 1, } \Lambda_5 = 107\ \text{MeV: } \sigma(k_T > 32\ GeV,\ |y| < 1.5) &= .00169\ \mu\mathrm{b} \\
\text{MRS set 2, } \Lambda_5 = 250\ \text{MeV: } \sigma(k_T > 32\ GeV,\ |y| < 1.5) &= .00315\ \mu\mathrm{b} \\
\text{MRS set 3, } \Lambda_5 = 178\ \text{MeV: } \sigma(k_T > 32\ GeV,\ |y| < 1.5) &= .00188\ \mu\mathrm{b}. \qquad (6.2)
\end{aligned}$$

With MRS set 1 and 3, the prediction lies inside the error band of fig. 14 and table 7. With MRS set 2 we get a somewhat higher value, although not high enough to be in agreement with the UA1 data point. We attribute this difference to the fact that the set 2 has a parametrisation of the gluon structure function much harder than the other two. This is somewhat in contrast with direct photon data[25]. Fig. 15 shows our prediction for the analogous quantity at the energy of the Tevatron.

In figs. 16 and 17 we show the y and k_T distribution of charm in proton antiproton collisions. The prediction of the charm cross sections at collider energies is controlled by the low x region of the gluon distributions. We shall return in the following subsection to the problem of predicting charm cross sections. It should be apparent to the reader that figs. 16 and 17 can at best give qualitative information about the charm cross-section.

6.2. Fixed target energies

The majority of the data on heavy quark production refers to charm quark production at fixed target energies. The analysis of the effect of the radiative corrections in charm production is very difficult. Although it is in practice very easy to calculate cross sections using some parametrisation of the structure functions, with a given choice of the subtraction scale, it is extremely difficult to estimate the reliability of the results. The problem originates from the smallness of the charm quark mass. If we choose $\mu = \sqrt{(k_T^2 + m_c^2)/2}$ in order to estimate the scale sensitivity of the result, at low k_T we obtain $\mu = .7 - .8$ GeV. Most parametrisations of the structure functions require $\mu \geq 3$ GeV. If one tries to evolve the structure functions backwards, to reach such a low scale, one encounters instabilities in the evolution equation. Nevertheless, it is interesting to examine the qualitative effects of the inclusion of the radiative corrections. We make no attempt to give estimates of the theoretical errors. We will always use the DFLM structure functions, with $\Lambda_4 = 260$ MeV, $\mu = 2\sqrt{(m_c^2 + k_T^2)}$ and $m_c = 1.5$ GeV. We stress that in all cases errors will be very large, and their estimate very difficult, so that our results will at best have a qualitative significance.

It is interesting to see if the radiative corrections provide for any enhancement in the large x_F region in proton-proton collisions. In fig. 18 we show the full $O(\alpha_S^3)$ differential distribution in x_F for three typical values of the centre of mass energy. No large enhancement is predicted at large x_F. This conclusion was already reached in ref. [7]. In the range $0.1 < x_F < 0.6$ the x_F behaviour is consistent with $(1 - x_F)^n$ for n between 6 and 7.5. In fig. 19, we show the k_T distribution for positive x_F.

The experimental results on the x_F distribution of charmed hadrons are in conflict. Some ISR experiments[26] report very large cross sections for charmed baryon production in the forward direction. On the other hand, fixed target experiments[29] and other ISR experiments[27] do not observe such an effect. It is clear that the result of fig. 18 cannot justify the results of ref. [26].

In lowest order QCD, there is no difference between heavy quark and heavy antiquark production. When radiative corrections are included, there is a difference, which comes from the subprocesses $qg \to Q(\bar{Q})+X$, and $q\bar{q} \to Q(\bar{Q})+X$. Examples of interference diagrams responsible for the charge asymmetry are shown in fig. 20. These effects will be largest in processes which involve predominantly the quark or antiquark distributions. It is therefore natural to look for these effects in pion induced processes. In fig. 21, we show the x_F distribution of c and $\bar{c}$ production in $\pi^- P$ collisions. The small difference between the c and $\bar{c}$ distributions comes mostly from the $q\bar{q}$ annihilation subprocess. The effect becomes more pronounced as x_F grows. For example, at $x_F = 0.4,\ 0.6,\ 0.8$ the cross sections for the production of a $\bar{c}$ are larger than the cross sections for the production of a c by factors of 1.04, 1.1, 1.15 respectively.

This effect should not be confused with the so called leading particle effect. In $\pi^- N$ collisions the leading mesons are D^-, D^0, which carry an anti-charm and a charm quark respectively. The charge asymmetry will manifest itself as a difference of the total D^-, $\overline{D}^0$ production, minus the D^+, D^0 production.

If the leading particle effect is as large as reported in ref. [28] (with very small statistics), this charge asymmetry will be completely washed out. On the other hand, if the effect is as reported in ref. [29] then the charge asymmetry may be visible in a high statistics experiment.

The expectations for total bottom production cross section at fixed target energies are shown in fig. 22. The corresponding curve for pion induced bottom production is shown in fig. 23. Note that at lower energies pion beams are more efficient than proton beams for producing bottom quarks, even when the energy degradation inherent in producing a secondary beam is taken into account[30].

The x_F distributions of the produced bottom quarks are shown in fig. 24. We predict that $\bar{b}$ quarks are more copiously produced than b quarks in the large x_F region. The observability of these effects is a matter of experimental detail. In figs. 25 and 26 we show the differential distributions for bottom production in pN collisions at $\sqrt{S} = 40$ GeV and pp collisions at $\sqrt{S} = 62$ GeV.

7. Conclusions

The calculation of the radiative corrections has allowed us to make more reliable predictions for heavy quark differential distributions in hadronic collisions. In general we find that the shapes of the lowest order predictions are not appreciably altered by the inclusion of the first radiative correction.

Our results are most accurate for the case of the top quark. The differential distributions of top quarks are well predicted by perturbative QCD.

Bottom production cross sections are subject to larger theoretical errors. Our prediction for bottom production at the CERN collider agrees well with experimental results, except at the largest values of k_T. We have analysed the theoretical problems one encounters in heavy quark differential distributions at very high k_T.

In charm hadroproduction, the theoretical errors are even larger and hard to estimate. The general effect of our prediction is to increase the value of the cross section by a constant factor. We do not see an enhancement of the cross section in the large x_F region of the magnitude necessary to explain the cross section for Λ_c production observed at the ISR. We also show that there is a charge asymmetry for charm and bottom production in pion induced collisions which may be measurable.

Acknowledgement

We would like to acknowledge useful discussions with many colleagues including G. Altarelli, J. C. Collins, G. Martinelli, A. H. Mueller, F. Paige and D. E. Soper. One of us (RKE) would like to thank the theory group at ETH in Zurich for their kind hospitality during the completion of this paper.

References

[1] P. Nason, S. Dawson and R. K. Ellis, *Nucl. Phys.* **B303** (1988) 607 .

[2] P. Nason, Proceedings of the XXIV International Conference on High Energy Physics, R. Kotthaus and J. H. Kühn (eds.);
R. K. Ellis, Proceedings of the 7th Topical Workshop on Proton Antiproton Physics, June 20-24 1988, Fermilab-Conf-88/184-T;

P. Nason, Les Rencontres de Physique de la Vallée d'Aoste, La Thuile, February 26-March 5 1988.

[3] R. K. Ellis and P. Nason, *Nucl. Phys.* **B312** (1989) 551 .

[4] P. Nason, S. Dawson and R. K. Ellis, to be published.

[5] W. Beenakker, H. Kuijf, W. L. van Neerven and J. Smith, Leiden preprint (November 1988).

[6] F. Halzen, P. Hoyer and C. S. Kim, *Phys. Lett.* **195B** (1987) 74 .

[7] R. K. Ellis, in Strong Interactions in Gauge Theories, ed. J. Tran Thanh Van, editions Frontière, Gif-sur-Yvette, 1986 p.339.

[8] G. Altarelli *et al.*, *Nucl. Phys.* **B308** (1988) 724 .

[9] M. Gluck, J. F. Owens and E. Reya, *Phys. Rev.* **D17** (1978) 2324
B. L. Combridge, *Nucl. Phys.* **B151** (1979) 429

[10] G. Altarelli and G. Parisi, *Nucl. Phys.* **B126** (1977) 298 .

[11] E. C. Poggio, H. R. Quinn and S. Weinberg, *Phys. Rev.* **D13** (1976) 1958 .

[12] J. Collins, F. Wilczek and A. Zee, *Phys. Rev.* **D18** (1978) 242 ;
W. J. Marciano, *Phys. Rev.* **D29** (1984) 580 .

[13] W. A. Bardeen *et al.*, *Phys. Rev.* **D18** (1978) 3998 .

[14] J. C. Collins and D. E. Soper, *Ann. Rev. Nucl. Part. Sci.* **37** (1987) 383 and references therein.

[15] J. C. Collins and Wu-Ki Tung, *Nucl. Phys.* **B278** (1986) 934 .

[16] J. C. Collins, D. E. Soper and G. Sterman, *Nucl. Phys.* **B263** (1986) 37 .

[17] G. Altarelli, R. K. Ellis and G. Martinelli, *Nucl. Phys.* **B242** (1984) 120 .

[18] W. Furmanski and R. Petronzio, *Zeit. Phys.* **C11** (1982) 293 .

[19] B. L. Combridge, J. Kripfganz and J. Ranft, *Phys. Lett.* **70B** (1977) 234 .

[20] F. Aversa, J. Chiappetta, M. Greco and J. Guillet, Marseille preprint, CPT-88/P.2186, (December 1988).

[21] R. K. Ellis *et al.*, *Nucl. Phys.* **B173** (1980) 397 .

[22] M. Diemoz *et al.*, *Zeit. Phys.* **C39** (1988) 21 ;
J. V. Allaby *et al.*, *Phys. Lett.* **197B** (1987) 281 .

[23] A. D. Martin, R. G. Roberts and W. J. Stirling, *Phys. Lett.* **207B** (1988) 205 , RAL preprint 88-113, (December 1988).

[24] C. Albajar *et al.*, *Phys. Lett.* **213B** (1988) 405 ;
I. R. Kenyon, Proceedings of the XXIV International Conference on High Energy Physics, R. Kotthaus and J. H. Kühn (eds.).

[25] P. Aurenche *et al.*, LPTHE Orsay 88/38, LAPP TH-234/88, BI-TP 88/28 preprint.

[26] R608 collaboration, *Phys. Lett.* **199B** (1987) 304 ;
W. Lockman *et al.*, *Phys. Lett.* **85B** (1979) 443 ;
D. Drijard *et al.*, *Phys. Lett.* **85B** (1979) 452 ;
K. L. Giboni *et al.*, *Phys. Lett.* **85B** (1979) 437 ;
M. Basile *et al.*, *Lett. Nuovo Cimento* 30 (1981)481,487.

[27] A. G. Clark *et al.*, *Phys. Lett.* **77B** (1978) 339 ;
H. G. Fisher and W. M. Geist, *Zeit. Phys.* **C19** (1983) 159 .

[28] A. T. Goshaw, Proceedings of the Advanced Research Workshop on QCD Hard Hadronic Processes, St. Croix, Virgin Islands, Oct 8-13, 1987.

[29] ACCMOR coll., contributed paper to the XXIV International Conference on High Energy Physics, Munich, August 4-10,1988.

[30] R. K. Ellis and C. Quigg, Fermilab Note FN-445, January 1987, (unpublished).

Figure Captions

Fig. 1: The QCD picture of the inclusive production of a heavy quark in hadron-hadron collisions.

Fig. 2: The graphs contributing to the lowest order parton cross sections.

Fig. 3: Examples of graphs of contributing in order α_S^3 to the parton cross section.

Fig. 4: Graphs responsible for the $1/v$ singularity. The open circle stands for any lowest order graph.

Fig. 5: Graphs containing logarithmic singularities in the limit $m \to 0$. The open circle stands for any lowest order graph.

Fig. 6: The contributions of the three parton sub-processes to the differential cross section for $p\bar{p} \to Q+X$ with $m_Q = 40$ GeV and $\sqrt{S} = 630$ GeV. The three contributions are plotted versus k_T at zero rapidity. The structure functions of DFLM with $\Lambda_5 = 173$ MeV are used.

Fig. 7: Differential cross section for the hadronic production of a heavy quark with a mass of 40 GeV at $\sqrt{S} = 630$ GeV. The cross section is plotted versus k_T for different values of the rapidity. The dashed lines represent the lowest order contribution scaled by an arbitrary factor. The structure functions of DFLM with $\Lambda_5 = 173$ MeV are used.

Fig. 8: As in fig. 7 but with $m_Q = 80$ GeV.

Fig. 9: As in fig. 7 but with $m_Q = 40$ GeV and $\sqrt{S} = 1.8$ TeV.

Fig. 10: As in fig. 7 but with $m_Q = 80$ GeV and $\sqrt{S} = 1.8$ TeV.

Fig. 11: Differential cross section for $p\bar{p} \to Q + X$ with $m_Q = 5$ GeV at $\sqrt{S} = 630$ GeV. The cross section is plotted versus k_T for different values of the rapidity. The dashed lines represent the lowest order contribution scaled by an arbitrary factor. The structure functions of DFLM with $\Lambda_5 = 173$ MeV are used.

Fig. 12: As in fig. 11 but with $\sqrt{S} = 1.8$ TeV.

Fig. 13: Some diagrams of order α_S^4 that give enhanced contributions proportional to $\alpha_S^2(\alpha_S \ln(k_T/m))^2$ at high k_T. The open circle stands for any lowest order graph.

Fig. 14: Inclusive cross section for the production of a heavy quark with a mass of 4.75 GeV, with k_T and rapidity cuts, together with the corresponding experimental points from the UA1 experiment[24].

Fig. 15: Inclusive cross section for the production of a heavy quark with a mass of 4.75 GeV, with k_T and rapidity cuts at $\sqrt{S} = 1.8$ TeV.

Fig. 16: Rapidity distribution of inclusive charm quark production in $p\bar{p}$ collisions at CM energies of 630 and 1800 GeV. The upper curves refer to the higher energy.

Fig. 17: Distribution in k_T for inclusive charm quark production in $p\bar{p}$ collisions at CM energies of 630 and 1800 GeV. The upper curves refer to the higher energy.

Fig. 18: Distribution in x_F of inclusive charm quark production in proton proton collisions at CM energies of 27.4, 38.7, and 62 GeV. The upper curves refer to the higher energies.

Fig. 19: Distribution in k_T of inclusive charm quark production in proton proton collisions at CM energy of 27.4, 38.7, and 62 GeV, with $x_F > 0$. The upper curves refer to the higher energies.

Fig. 20: Examples of interference terms that contribute to the charge asymmetry in heavy quark and heavy antiquark production.

Fig. 21: Cross section for the production of c and $\bar{c}$ in $\pi^- p$ collisions vs. x_F.

Fig. 22: Total cross section for the production of bottom in pN collisions vs. beam energy.

Fig. 23: Total cross section for the production of bottom in πN collisions vs. beam energy.

Fig. 24: Cross section for the production of b and $\bar{b}$ in $\pi^- N$ collisions vs. x_F.

Fig. 25: Cross section for the production of bottom vs. x_F in pN collisions at $\sqrt{S} = 40$ GeV and pp collisions at $\sqrt{S} = 62$ GeV.

Fig. 26: Cross section for the production of bottom vs. k_T in pN collisions at $\sqrt{S} = 40$ GeV and pp collisions at $\sqrt{S} = 62$ GeV.

APPENDIX A:

The parton cross sections are available as a set of fortran functions. The routines for the gluon gluon subprocess are the following:

$$
\begin{aligned}
h^{(0)}_{gg}(\tau_1,\rho) &\rightarrow \texttt{HQHOGG(T1,RHO)} \\
h^{(d)}_{gg}(\tau_1,\rho) &\rightarrow \texttt{HQHDGG(T1,RHO,NL)} \\
\bar{h}^{(d)}_{gg}(\tau_1,\rho) &\rightarrow \texttt{HQBDGG(T1,RHO)} \\
h^{(+)}_{gg}(\tau_1,\tau_2,\rho) &\rightarrow \texttt{HQHPGG(TX,T1,RHO)} \\
\bar{h}^{(+)}_{gg}(\tau_1,\tau_2,\rho) &\rightarrow \texttt{HQBPGG(TX,T1,RHO)} \\
h^{(l)}_{gg}(\tau_1,\tau_2,\rho) &\rightarrow \texttt{HQHLGG(TX,T1,RHO)}
\end{aligned} \tag{A.1}
$$

in an obvious notation where $\texttt{T1} = \tau_1, \texttt{TX} = \tau_x = 1-\tau_1-\tau_2, \texttt{RHO} = \rho$ and $\texttt{NL} = n_{lf}$. Analogous routines are available for the other subprocesses, according to the notation convention G for gluon, Q for quark, A for antiquark. In the processes involving initial quarks, the charge symmetric and charge antisymmetric contributions are given by separate routines. Therefore:

$$
\begin{aligned}
h^{(d)}_{q\bar{q}}(\tau_1,\rho) &\rightarrow \texttt{HQHDQA(T1,RHO,NL) + ASHDQA(T1,RHO)} \\
h^{(+)}_{q\bar{q}}(\tau_1,\tau_2,\rho) &\rightarrow \texttt{HQHPQA(TX,T1,RHO) + ASHPQA(TX,T1,RHO)} \\
h^{(d)}_{\bar{q}q}(\tau_1,\rho) &\rightarrow \texttt{HQHDQA(T1,RHO) - ASHDQA(T1,RHO)} \\
h^{(+)}_{\bar{q}q}(\tau_1,\tau_2,\rho) &\rightarrow \texttt{HQHPQA(TX,T1,RHO) - ASHPQA(TX,T1,RHO)} \\
h^{(+)}_{qg}(\tau_1,\tau_2,\rho) &\rightarrow \texttt{HQHPQG(TX,T1,RHO) + ASHPQG(TX,T1,RHO)} \\
h^{(+)}_{\bar{q}g}(\tau_1,\tau_2,\rho) &\rightarrow \texttt{HQHPQG(TX,T1,RHO) - ASHPQG(TX,T1,RHO)}
\end{aligned} \tag{A.2}
$$

There are also fortran functions which return the various correction terms which are appropriate for use in factorisation schemes other than $\overline{\text{MS}}$. We have

$$
\begin{aligned}
h'^{(d)}_{gg} - h^{(d)}_{gg} &\rightarrow \texttt{CTHDGG(T1,RHO,NL)} \\
h'^{(d)}_{q\bar{q}} - h^{(d)}_{gg} &\rightarrow \texttt{CTHDQA(T1,RHO,NL)} \\
h'^{(d)}_{qg} - h^{(d)}_{gg} &\rightarrow \texttt{CTHDQG(T1,RHO,NL)}
\end{aligned}
$$

$$h'^{(+)}_{gg} - h^{(d)}_{gg} \rightarrow \texttt{CTHPGG(TX,T1,RHO,NL)}$$

$$h'^{(+)}_{q\bar{q}} - h^{(d)}_{gg} \rightarrow \texttt{CTHPQA(TX,T1,RHO,NL)}$$

$$h'^{(+)}_{qg} - h^{(d)}_{gg} \rightarrow \texttt{CTHPQG(TX,T1,RHO,NL)}. \tag{A.3}$$

The above functions invoke other functions, which give the values of the function K in Sec. IV:

$$
\begin{aligned}
K^{(d)}_{gg}(x, n_{\rm lf}) &\rightarrow \texttt{XKDGG(NL)} \\
K^{(+)}_{gg}(x, n_{\rm lf}) &\rightarrow \texttt{XKPGG(X,NL)} \\
K^{(l)}_{gg}(x, n_{\rm lf}) &\rightarrow \texttt{XKLGG(X,NL)} \\
K^{(d)}_{qq}(x, n_{\rm lf}) &\rightarrow \texttt{XKDQQ(NL)} \\
K^{(+)}_{qq}(x, n_{\rm lf}) &\rightarrow \texttt{XKPQQ(X,NL)} \\
K^{(l)}_{qq}(x, n_{\rm lf}) &\rightarrow \texttt{XKLQQ(X,NL)} \\
K^{(d)}_{qg}(x, n_{\rm lf}) &\rightarrow \texttt{XKDQG(NL)} \\
K^{(+)}_{qg}(x, n_{\rm lf}) &\rightarrow \texttt{XKPQG(X,NL)} \\
K^{(l)}_{qg}(x, n_{\rm lf}) &\rightarrow \texttt{XKLQG(X,NL)}
\end{aligned} \tag{A.4}
$$

The above functions are given for the particular definition of the parton densities of ref. [17]. They should be appropriately changed in order to use other definitions. A full list of the routines is given in Table 8.

$\frac{d\sigma}{dy dk_T^2}$ (pb/GeV^2) $\sqrt{S}=630$ GeV, $m_t=40$ GeV, $\Lambda_5=173$ MeV, $\mu=\mu_0=\sqrt{k_T^2+m_t^2}$.								
k_T (GeV)	y	$\frac{d\sigma}{dy dk_T^2}$ (pb/GeV^2)	μ		Λ_5 (MeV)		$+\Delta$	$-\Delta$
			$\mu_0/2$	$2\mu_0$	101	250		
.8	0	.477	.098	-.088	-.098	.022	.1	-.132
	.55	.403	.081	-.075	-.086	.023	.084	-.114
	1.1	.229	.046	-.043	-.053	.020	.05	-.069
	1.65	$.71\times10^{-1}$	.173	-.149	-.182	.088	.194	-.235
	2.2	$.577\times10^{-2}$	.297	-.17	-.134	.028	.298	-.216
8	0	.427	.08	-.077	-.088	.024	.084	-.117
	.55	.362	.069	-.066	-.077	.023	.072	-.102
	1.1	.206	.042	-.039	-.048	.018	.046	-.062
	1.65	$.618\times10^{-1}$	.159	-.134	-.159	.075	.176	-.208
	2.2	$.459\times10^{-2}$	.24	-.136	-.104	.015	.24	-.171
16	0	.303	.054	-.055	-.064	.017	.057	-.084
	.55	.254	.046	-.047	-.055	.016	.049	-.072
	1.1	.14	.028	-.027	-.033	.012	.031	-.043
	1.65	$.382\times10^{-1}$	.102	-.086	-.098	.046	.112	-.131
	2.2	$.235\times10^{-2}$	.126	-.073	-.053	-.002	.126	-.090
24	0	.177	.03	-.032	-.038	.011	.032	-.050
	.55	.146	.025	-.027	-.032	.010	.027	-.042
	1.1	$.758\times10^{-1}$	.148	-.15	-.181	.068	.163	-.235
	1.65	$.181\times10^{-1}$	.05	-.043	-.047	.020	.054	-.063
	2.2	$.778\times10^{-3}$	.455	-.267	-.183	-.032	.455	-.324
32	0	$.904\times10^{-1}$	.14	-.164	-.199	.058	.151	-.258
	.55	$.732\times10^{-1}$	.118	-.136	-.165	.051	.129	-.214
	1.1	$.353\times10^{-1}$	.066	-.07	-.085	.032	.073	-.111
	1.65	$.699\times10^{-2}$	.198	-.172	-.177	.063	.208	-.247
	2.2	$.158\times10^{-3}$	.105	-.061	-.04	-.013	.105	-.073
40	0	$.432\times10^{-1}$	.06	-.076	-.096	.029	.067	-.123
	.55	$.343\times10^{-1}$	.05	-.061	-.078	.025	.056	-.099
	1.1	$.152\times10^{-1}$	.026	-.03	-.037	.013	.029	-.047
	1.65	$.237\times10^{-2}$	.067	-.058	-.058	.014	.069	-.082
	2.2	$.145\times10^{-4}$	.111	-.061	-.042	-.020	.111	-.074
48	0	$.203\times10^{-1}$	.025	-.034	-.045	.014	.029	-.057
	.55	$.156\times10^{-1}$	.02	-.027	-.036	.011	.023	-.045
	1.1	$.631\times10^{-2}$	.098	-.119	-.15	.048	.109	-.192
	1.65	$.735\times10^{-3}$	.198	-.176	-.17	.012	.198	-.245
	2.2	$.174\times10^{-6}$	.152	-.085	-.065	-.037	.152	-.107

Table 1: Differential cross section for top production, with $\sqrt{S}=630$ GeV, $m_t=40$ GeV, for various values of k_T and the rapidity y. Columns 4–7 give the variation of the result when one of the parameters μ, Λ_5, is changed from its central value as indicated above the column. The appropriate power of ten, shown explicitly in column 3, is understood in columns 4–9. The quantity $+\Delta$ $(-\Delta)$ is sum in quadrature of all the positive (negative) errors in columns 4–7.

$\frac{d\sigma}{dy dk_T^2}$ (pb/GeV^2) $\sqrt{S} = 630$ GeV, $m_t = 80$ GeV, $\Lambda_5 = 173$ MeV, $\mu = \mu_0 = \sqrt{k_T^2 + m_t^2}$.								
k_T (GeV)	y	$\frac{d\sigma}{dy dk_T^2}$ (pb/GeV^2)	μ		Λ_5 (MeV)		$+\Delta$	$-\Delta$
			$\mu_0/2$	$2\mu_0$	101	250		
1.6	0	$.37 \times 10^{-2}$	.017	-.044	-.076	.016	.024	-.088
	.41	$.308 \times 10^{-2}$	.017	-.038	-.064	.013	.021	-.074
	.82	$.169 \times 10^{-2}$	.013	-.023	-.036	.006	.015	-.043
	1.23	$.488 \times 10^{-3}$	.072	-.085	-.107	.004	.072	-.136
	1.64	$.321 \times 10^{-4}$	.09	-.077	-.077	-.024	.09	-.109
16	0	$.354 \times 10^{-2}$	.035	-.05	-.073	.016	.039	-.089
	.41	$.291 \times 10^{-2}$	.03	-.042	-.061	.013	.032	-.074
	.82	$.153 \times 10^{-2}$	.018	-.023	-.033	.005	.019	-.040
	1.23	$.398 \times 10^{-3}$	.063	-.07	-.087	.001	.063	-.112
	1.64	$.229 \times 10^{-4}$	.067	-.056	-.056	-.019	.067	-.079
32	0	$.231 \times 10^{-2}$	.025	-.033	-.048	.010	.027	-.058
	.41	$.187 \times 10^{-2}$	.021	-.027	-.039	.007	.022	-.048
	.82	$.925 \times 10^{-3}$	.12	-.144	-.198	.024	.122	-.245
	1.23	$.212 \times 10^{-3}$	.037	-.038	-.047	-.003	.037	-.060
	1.64	$.789 \times 10^{-5}$	.261	-.199	-.203	-.085	.261	-.284
48	0	$.117 \times 10^{-2}$	.014	-.017	-.025	.004	.014	-.030
	.41	$.929 \times 10^{-3}$	.111	-.135	-.196	.024	.113	-.238
	.82	$.424 \times 10^{-3}$	.058	-.066	-.092	.004	.058	-.113
	1.23	$.787 \times 10^{-4}$	.143	-.14	-.174	-.031	.143	-.223
	1.64	$.114 \times 10^{-5}$	.044	-.03	-.032	-.018	.044	-.044
64	0	$.507 \times 10^{-3}$	.059	-.072	-.106	.008	.059	-.128
	.41	$.389 \times 10^{-3}$	.047	-.056	-.082	.004	.047	-.099
	.82	$.158 \times 10^{-3}$	.022	-.024	-.034	-.002	.022	-.042
	1.23	$.216 \times 10^{-4}$	.041	-.039	-.049	-.015	.041	-.063
	1.64	$.348 \times 10^{-7}$	.153	-.097	-.114	-.089	.153	-.150

Table 2: Differential cross section for top production, with $\sqrt{S} = 630$ GeV, $m_t = 80$ GeV. The meaning of the quoted errors is as in Table 1.

$\frac{d\sigma}{dy dk_T^2}$ (pb/GeV^2) $\sqrt{S} = 1800$ GeV, $m_t = 40$ GeV, $\Lambda_5 = 173$ MeV, $\mu = \mu_0 = \sqrt{k_T^2 + m_t^2}$.								
k_T (GeV)	y	$\frac{d\sigma}{dy dk_T^2}$ (pb/GeV^2)	μ: $\mu_0/2$	μ: $2\mu_0$	Λ_5 (MeV): 101	Λ_5 (MeV): 250	$+\Delta$	$-\Delta$
.8	0	$.413 \times 10^1$	.09	-.076	-.056	.001	.09	-.094
	.76	$.353 \times 10^1$	.078	-.065	-.052	.005	.078	-.083
	1.52	$.208 \times 10^1$	.047	-.039	-.039	.013	.049	-.055
	2.28	.672	.161	-.131	-.172	.114	.197	-.216
	3.04	$.559 \times 10^{-1}$	.233	-.156	-.174	.161	.283	-.234
8	0	$.357 \times 10^1$	.07	-.062	-.048	.001	.07	-.078
	.76	$.306 \times 10^1$	.061	-.053	-.044	.004	.061	-.069
	1.52	$.182 \times 10^1$	.038	-.033	-.033	.011	.039	-.047
	2.28	.588	.138	-.115	-.15	.098	.169	-.189
	3.04	$.458 \times 10^{-1}$	.197	-.131	-.142	.129	.236	-.193
16	0	$.267 \times 10^1$	.049	-.045	-.035	-.001	.049	-.058
	.76	$.228 \times 10^1$	.043	-.039	-.033	.002	.043	-.051
	1.52	$.132 \times 10^1$	.026	-.024	-.024	.008	.027	-.034
	2.28	.401	.093	-.08	-.104	.068	.116	-.131
	3.04	$.257 \times 10^{-1}$	.123	-.081	-.078	.066	.139	-.113
24	0	$.17 \times 10^1$	.031	-.029	-.023	-.002	.031	-.037
	.76	$.143 \times 10^1$	.026	-.025	-.021	.001	.026	-.033
	1.52	.797	.157	-.145	-.153	.044	.163	-.211
	2.28	.22	.052	-.046	-.058	.038	.064	-.074
	3.04	$.105 \times 10^{-1}$	.057	-.035	-.029	.021	.061	-.046
32	0	.961	.173	-.166	-.134	-.014	.173	-.213
	.76	.797	.146	-.14	-.122	.000	.146	-.186
	1.52	.423	.083	-.079	-.084	.024	.086	-.115
	2.28	.103	.025	-.022	-.028	.018	.031	-.036
	3.04	$.356 \times 10^{-2}$	.203	-.12	-.083	.034	.206	-.145
40	0	.506	.092	-.089	-.074	-.008	.092	-.116
	.76	.414	.076	-.074	-.066	.000	.076	-.100
	1.52	.208	.041	-.039	-.043	.012	.042	-.058
	2.28	$.438 \times 10^{-1}$	.11	-.099	-.12	.076	.134	-.156
	3.04	$.108 \times 10^{-2}$	.063	-.038	-.024	.002	.063	-.045
48	0	.26	.047	-.046	-.04	-.004	.047	-.061
	.76	.209	.038	-.038	-.035	.000	.038	-.052
	1.52	$.99 \times 10^{-1}$	.192	-.191	-.212	.060	.201	-.285
	2.28	$.178 \times 10^{-1}$	.045	-.041	-.049	.030	.054	-.064
	3.04	$.254 \times 10^{-3}$	.164	-.097	-.059	-.011	.164	-.114
60	0	$.962 \times 10^{-1}$	.179	-.173	-.161	-.011	.179	-.236
	.76	$.757 \times 10^{-1}$	.143	-.138	-.137	.004	.143	-.195
	1.52	$.327 \times 10^{-1}$	.066	-.063	-.074	.021	.069	-.097
	2.28	$.433 \times 10^{-2}$	.131	-.107	-.118	.064	.145	-.159
	3.04	$.107 \times 10^{-4}$	.091	-.048	-.028	-.017	.091	-.055

Table 3: Differential cross section for top production, with $\sqrt{S} = 1800$ GeV, $m_t = 40$ GeV. The meaning of the quoted errors is as in Table 1.

$\frac{d\sigma}{dy\,dk_T^2}$ (pb/GeV^2)								
$\sqrt{S} = 1800$ GeV, $m_t = 80$ GeV, $\Lambda_5 = 173$ MeV, $\mu = \mu_0 = \sqrt{k_T^2 + m_t^2}$.								
k_T (GeV)	y	$\frac{d\sigma}{dy\,dk_T^2}$ (pb/GeV^2)	μ		Λ_5 (MeV)		$+\Delta$	$-\Delta$
			$\mu_0/2$	$2\mu_0$	101	250		
1.6	0	$.439 \times 10^{-1}$	.08	-.074	-.075	.000	.08	-.106
	.62	$.371 \times 10^{-1}$	.066	-.063	-.067	.004	.067	-.092
	1.24	$.212 \times 10^{-1}$	.036	-.036	-.044	.010	.038	-.056
	1.87	$.647 \times 10^{-2}$	.125	-.119	-.156	.065	.141	-.196
	2.49	$.498 \times 10^{-3}$	.207	-.137	-.117	.029	.209	-.181
16	0	$.386 \times 10^{-1}$	.062	-.062	-.066	.003	.062	-.091
	.62	$.328 \times 10^{-1}$	.053	-.053	-.059	.005	.053	-.079
	1.24	$.189 \times 10^{-1}$	.031	-.031	-.039	.009	.033	-.050
	1.87	$.565 \times 10^{-2}$	.114	-.105	-.136	.056	.127	-.172
	2.49	$.397 \times 10^{-3}$	.168	-.109	-.09	.017	.169	-.141
32	0	$.278 \times 10^{-1}$	.043	-.044	-.049	.002	.044	-.066
	.62	$.234 \times 10^{-1}$	.037	-.037	-.043	.004	.037	-.057
	1.24	$.13 \times 10^{-1}$	.022	-.022	-.027	.006	.023	-.035
	1.87	$.365 \times 10^{-2}$	.077	-.069	-.089	.035	.085	-.112
	2.49	$.212 \times 10^{-3}$	.096	-.059	-.045	.001	.096	-.074
48	0	$.167 \times 10^{-1}$	.026	-.026	-.03	.001	.026	-.040
	.62	$.139 \times 10^{-1}$	.022	-.022	-.026	.003	.022	-.034
	1.24	$.734 \times 10^{-2}$	.126	-.121	-.158	.037	.131	-.199
	1.87	$.18 \times 10^{-2}$	.042	-.035	-.044	.016	.045	-.056
	2.49	$.816 \times 10^{-4}$	.403	-.238	-.173	-.035	.403	-.294
64	0	$.882 \times 10^{-2}$	.134	-.134	-.167	.011	.134	-.214
	.62	$.72 \times 10^{-2}$	.112	-.111	-.142	.016	.113	-.180
	1.24	$.358 \times 10^{-2}$	.063	-.058	-.079	.019	.065	-.098
	1.87	$.746 \times 10^{-3}$	.19	-.147	-.181	.058	.199	-.233
	2.49	$.213 \times 10^{-4}$	.123	-.067	-.048	-.018	.123	-.082
80	0	$.437 \times 10^{-2}$	.063	-.066	-.085	.008	.064	-.108
	.62	$.35 \times 10^{-2}$	.052	-.054	-.071	.010	.053	-.089
	1.24	$.163 \times 10^{-2}$	.028	-.027	-.036	.009	.029	-.045
	1.87	$.279 \times 10^{-3}$	.075	-.058	-.067	.016	.076	-.089
	2.49	$.362 \times 10^{-5}$	.244	-.126	-.089	-.050	.244	-.154
96	0	$.212 \times 10^{-2}$	.029	-.032	-.043	.006	.029	-.053
	.62	$.167 \times 10^{-2}$	.023	-.025	-.035	.006	.024	-.043
	1.24	$.717 \times 10^{-3}$	.117	-.118	-.161	.037	.123	-.200
	1.87	$.966 \times 10^{-4}$	.271	-.209	-.227	.031	.273	-.308
	2.49	$.266 \times 10^{-6}$	.219	-.106	-.077	-.058	.219	-.131

Table 4: Differential cross section for top production, with $\sqrt{S} = 1800$ GeV, $m_t = 80$ GeV. The meaning of the quoted errors is as in Table 1.

$\frac{d\sigma}{dy dk_T^2}$ (μb/GeV^2) $\sqrt{S} = 630$ GeV, $m_b = 4.75$ GeV, $\Lambda_5 = 173$ MeV, $\mu = \mu_0 = \sqrt{k_T^2 + m_b^2}$.											
k_T	y	$\frac{d\sigma}{dy dk_T^2}$	μ		Λ_5 (MeV)		m (GeV)		δ	$+\Delta$	$-\Delta$
(GeV)		(μb/GeV^2)	$\mu_0/2$	$2\mu_0$	101	250	4.5	5			
.01	0	.244	.074	-.041	-.068	.081	.077	-.056	0	.134	-.098
	1	.220	.070	-.040	-.064	.075	.071	-.052	0	.125	-.091
	2	.149	.054	-.032	-.048	.058	.053	-.037	0	.095	-.069
	3	$.567 \times 10^{-1}$	.231	-.143	-.231	.327	.243	-.164	0	.468	-.317
	4	$.489 \times 10^{-2}$	.198	-.150	-.270	.587	.303	-.183	0	.690	-.359
1	0	.198	.060	-.032	-.053	.062	.060	-.045	0	.105	-.076
	1	.178	.056	-.030	-.050	.057	.056	-.041	0	.098	-.071
	2	.121	.043	-.024	-.037	.044	.041	-.029	0	.074	-.053
	3	$.471 \times 10^{-1}$	.187	-.114	-.186	.254	.192	-.132	0	.369	-.255
	4	$.409 \times 10^{-2}$	.170	-.128	-.225	.490	.250	-.152	0	.576	-.300
3	0	.104	.028	-.019	-.024	.026	.025	-.020	-.001	.046	-.036
	1	$.912 \times 10^{-1}$	.266	-.171	-.224	.240	.223	-.178	-.007	.422	-.334
	2	$.581 \times 10^{-1}$	.196	-.122	-.166	.183	.153	-.119	-.005	.309	-.238
	3	$.194 \times 10^{-1}$	.079	-.048	-.075	.101	.061	-.045	-.002	.141	-.100
	4	$.106 \times 10^{-2}$	.056	-.037	-.056	.122	.050	-.035	-.001	.143	-.075
5	0	$.372 \times 10^{-1}$	.119	-.078	-.075	.067	.061	-.052	-.011	.149	-.120
	1	$.319 \times 10^{-1}$	.107	-.069	-.069	.062	.053	-.046	-.010	.135	-.108
	2	$.184 \times 10^{-1}$	.071	-.043	-.048	.048	.033	-.028	-.007	.091	-.071
	3	$.482 \times 10^{-2}$	.218	-.128	-.183	.240	.102	-.084	-.022	.339	-.240
	4	$.113 \times 10^{-3}$	.090	-.048	-.053	.104	.038	-.029	-.002	.143	-.077
10	0	$.255 \times 10^{-2}$	.110	-.066	-.043	.020	.018	-.017	-.027	.113	-.085
	1	$.203 \times 10^{-2}$	.090	-.053	-.038	.019	.015	-.014	-.023	.093	-.071
	2	$.886 \times 10^{-3}$	.417	-.242	-.223	.166	.068	-.066	-.123	.454	-.358
	3	$.999 \times 10^{-4}$	.532	-.305	-.388	.499	.093	-.076	-.154	.735	-.522
20	0	$.503 \times 10^{-4}$	.228	-.144	-.090	.013	.016	-.016	-.116	.229	-.206
	1	$.350 \times 10^{-4}$	.158	-.102	-.071	.019	.011	-.011	-.087	.159	-.152
	2	$.844 \times 10^{-5}$	.374	-.255	-.242	.162	.026	-.024	-.244	.408	-.429
	3	$.111 \times 10^{-6}$	.084	-.046	-.027	.012	.004	-.005	-.002	.085	-.053
40	0	$.434 \times 10^{-6}$	.179	-.116	-.100	.022	.008	-.008	-.134	.181	-.203
	1	$.227 \times 10^{-6}$	.091	-.060	-.057	.019	.004	-.003	-.073	.093	-.110
	2	$.123 \times 10^{-7}$	.057	-.036	-.033	.015	.001	-.001	-.023	.059	-.054
60	0	$.203 \times 10^{-7}$	.050	-.044	-.048	.013	.002	-.002	-.054	.052	-.085
	1	$.771 \times 10^{-8}$	.160	-.162	-.191	.061	.005	-.004	-.198	.171	-.319
	2	$.535 \times 10^{-10}$	.221	-.166	-.128	-.053	0	0	-.030	.221	-.212
80	0	$.199 \times 10^{-8}$	.023	-.030	-.045	.009	.001	-.001	-.038	.025	-.066
	1	$.513 \times 10^{-9}$	.023	-.069	-.114	.013	-.001	.001	-.083	.026	-.157

Table 5: Differential cross section for bottom production, for various values of k_T and the rapidity y. Columns 4 through 9 give the variation of the result when one of the parameters μ, Λ_5, or m_b, is changed from its central value, as indicated above the column. The quantity δ represents the effect of some terms of the order $\alpha_S^2(\alpha_S \ln(k_T/m_b))^2$. The quantity $+\Delta$ ($-\Delta$) is the sum in quadrature of all the positive (negative) errors in columns 4 through 10.

$\frac{d\sigma}{dy\,dk_T^2}$ (μb/GeV^2)

$\sqrt{S} = 1800$ GeV, $m_b = 4.75$ GeV, $\Lambda_5 = 173$ MeV, $\mu = \mu_0 = \sqrt{k_T^2 + m_b^2}$.

k_T (GeV)	y	$\frac{d\sigma}{dy\,dk_T^2}$ (μb/GeV^2)	μ: $\mu_0/2$	μ: $2\mu_0$	Λ_5 (MeV): 101	Λ_5 (MeV): 250	m (GeV): 4.5	m (GeV): 5	δ	$+\Delta$	$-\Delta$
.01	0	.554	.063	-.039	-.215	.348	.156	-.117	0	.386	-.248
	1	.529	.069	-.044	-.207	.329	.152	-.114	0	.369	-.240
	3	.297	.070	-.048	-.128	.197	.100	-.072	0	.232	-.155
	4	.115	.034	-.024	-.057	.100	.047	-.032	0	.116	-.070
	5	$.994 \times 10^{-2}$	.315	-.261	-.621	1.548	.676	-.319	0	1.718	-.745
1	0	.459	.063	-.033	-.172	.274	.125	-.095	0	.307	-.199
	1	.437	.067	-.035	-.165	.259	.121	-.091	0	.293	-.192
	3	.241	.059	-.037	-.101	.153	.078	-.057	0	.182	-.121
	4	$.950 \times 10^{-1}$	.280	-.191	-.463	.785	.369	-.258	0	.911	-.563
	5	$.794 \times 10^{-2}$	.263	-.208	-.493	1.229	.560	-.222	0	1.375	-.579
3	0	.257	.036	-.026	-.085	.130	.056	-.046	-.002	.146	-.100
	1	.242	.038	-.026	-.081	.122	.054	-.043	-.002	.139	-.096
	3	.120	.031	-.019	-.046	.068	.030	-.024	-.001	.081	-.056
	4	$.406 \times 10^{-1}$	.135	-.082	-.191	.320	.122	-.092	-.005	.368	-.228
	5	$.247 \times 10^{-2}$	.101	-.070	-.149	.387	.111	-.075	-.003	.415	-.181
5	0	.106	.021	-.015	-.030	.042	.017	-.014	-.003	.049	-.036
	1	$.979 \times 10^{-1}$	.206	-.143	-.281	.386	.154	-.132	-.031	.463	-.344
	3	$.414 \times 10^{-1}$	.130	-.078	-.145	.196	.072	-.061	-.018	.246	-.177
	4	$.109 \times 10^{-1}$	.042	-.024	-.049	.081	.023	-.019	-.006	.094	-.059
	5	$.299 \times 10^{-3}$	.177	-.107	-.166	.401	.100	-.075	-.008	.450	-.211
10	0	$.104 \times 10^{-1}$	.034	-.021	-.021	.022	.007	-.007	-.011	.041	-.033
	1	$.923 \times 10^{-2}$	.315	-.194	-.196	.199	.067	-.063	-.104	.379	-.301
	3	$.245 \times 10^{-2}$	.102	-.058	-.076	.085	.019	-.018	-.040	.135	-.105
	4	$.280 \times 10^{-3}$	.131	-.074	-.124	.201	.027	-.026	-.054	.241	-.157
	5	$.957 \times 10^{-7}$	1.187	-.474	-.360	.213	.350	-.489	-.001	1.255	-.770
20	0	$.346 \times 10^{-3}$	.141	-.084	-.055	.028	.012	-.012	-.077	.144	-.127
	1	$.288 \times 10^{-3}$	.119	-.072	-.050	.026	.010	-.010	-.068	.122	-.111
	3	$.315 \times 10^{-4}$	.136	-.088	-.100	.100	.011	-.011	-.114	.170	-.176
	4	$.410 \times 10^{-6}$	.255	-.157	-.131	.157	.013	-.011	-.018	.299	-.205
40	0	$.600 \times 10^{-5}$	.261	-.164	-.096	.007	.014	-.014	-.199	.261	-.276
	1	$.446 \times 10^{-5}$	.198	-.123	-.080	.014	.010	-.010	-.160	.198	-.217
	3	$.645 \times 10^{-7}$	.345	-.206	-.209	.182	.009	-.008	-.254	.390	-.388
80	0	$.588 \times 10^{-7}$	.250	-.160	-.117	.003	.010	-.010	-.237	.250	-.310
	1	$.355 \times 10^{-7}$	.149	-.096	-.078	.012	.006	-.006	-.155	.149	-.198
	3	$.669 \times 10^{-12}$	.737	-.330	-.203	-.183	.006	-.006	-.009	.737	-.387
160	0	$.321 \times 10^{-9}$	.088	-.068	-.073	.010	.003	-.003	-.111	.089	-.150
	1	$.123 \times 10^{-9}$	.028	-.024	-.029	.005	.001	-.001	-.043	.029	-.057

Table 6: Differential cross section for bottom production at a centre of mass energy of 1800 GeV. The notation is as explained in Table 5.

$\sigma(p\bar{p} \to b + X,\ \lvert y\rvert < y_{\max},\ k_T > k_{\min})$ (μb) $\sqrt{S} = 630$ GeV, $m_b = 4.75$ GeV, $\Lambda_5 = 173$ MeV, $\mu = \mu_0 = \sqrt{k_{\min}^2 + m_b^2}$.											
$k_{\min}$	$y_{\max}$	σ	μ		Λ_5 (MeV)		m (GeV)		δ	$+\Delta$	$-\Delta$
(GeV)		(μb)	$\mu_0/2$	$2\mu_0$	101	250	4.5	5			
0	1.5	$.103 \times 10^{2}$	.047	-.022	-.026	.026	.022	-.017	-.003	.058	-.038
	all y	$.156 \times 10^{2}$	.072	-.035	-.043	.046	.036	-.028	-.005	.093	-.062
1	1.5	$.96 \times 10^{1}$	.432	-.208	-.24	.237	.199	-.159	-.031	.531	-.356
	all y	$.145 \times 10^{2}$	.066	-.033	-.04	.042	.032	-.025	-.004	.085	-.058
5	1.5	$.287 \times 10^{1}$	.128	-.073	-.059	.044	.034	-.03	-.019	.14	-.101
	all y	$.399 \times 10^{1}$	.183	-.104	-.091	.075	.049	-.044	-.027	.204	-.147
6	1.5	$.192 \times 10^{1}$	.088	-.051	-.038	.026	.019	-.017	-.015	.094	-.068
	all y	$.261 \times 10^{1}$	.122	-.07	-.057	.043	.027	-.024	-.021	.132	-.096
6.5	1.5	$.157 \times 10^{1}$	.073	-.042	-.031	.019	.014	-.013	-.014	.077	-.056
	all y	$.211 \times 10^{1}$	.1	-.057	-.046	.033	.02	-.018	-.018	.107	-.077
10	1.5	$.41 \times 10^{0}$	.202	-.116	-.078	.033	.023	-.022	-.055	.206	-.152
	all y	$.515 \times 10^{0}$	.255	-.146	-.106	.055	.03	-.028	-.069	.263	-.195
15	1.5	$.815 \times 10^{-1}$	.389	-.241	-.161	.049	.031	-.029	-.15	.394	-.328
	all y	$.96 \times 10^{-1}$	.46	-.286	-.2	.076	.036	-.035	-.177	.467	-.393
20	1.5	$.216 \times 10^{-1}$	.097	-.063	-.046	.012	.006	-.006	-.046	.098	-.091
	all y	$.243 \times 10^{-1}$	.109	-.072	-.053	.017	.007	-.007	-.052	.11	-.103
23	1.5	$.107 \times 10^{-1}$	.048	-.031	-.024	.006	.003	-.003	-.024	.048	-.046
	all y	$.119 \times 10^{-1}$	.053	-.034	-.027	.008	.003	-.003	-.026	.053	-.051
30	1.5	$.259 \times 10^{-2}$	.111	-.068	-.061	.017	.005	-.005	-.059	.113	-.11
	all y	$.277 \times 10^{-2}$	.119	-.073	-.066	.02	.005	-.005	-.063	.121	-.117
32	1.5	$.181 \times 10^{-2}$	.076	-.047	-.043	.012	.003	-.003	-.041	.077	-.076
	all y	$.191 \times 10^{-2}$	.08	-.049	-.046	.014	.004	-.003	-.043	.082	-.08
40	1.5	$.501 \times 10^{-3}$	.171	-.121	-.123	.038	.007	-.007	-.107	.176	-.203
	all y	$.519 \times 10^{-3}$	.178	-.126	-.128	.04	.007	-.007	-.11	.183	-.21

Table 7: Cross section for inclusive bottom production, with transverse momentum and rapidity cuts. Columns 4 through 9 give the variation of the result when one of the parameters μ, Λ_5, or m_b, is changed from its central value, as indicated above the column. The quantity δ represents the effect of some terms of the order $\alpha_S^2(\alpha_S \ln(k_T/m_b))^2$. The quantity $+\Delta$ ($-\Delta$) is the sum in quadrature of all the positive (negative) errors in columns 4 through 10.

ij	$h_{ij}^{(0)}$	$h_{ij}^{(d)}$	$\bar{h}_{ij}^{(d)}$	$h_{ij}^{(+)}$	$\bar{h}_{ij}^{(+)}$	$h_{ij}^{(l)}$
gg	HQHOGG	HQHDGG CTHDGG	HQBDGG	HQHPGG CTHPGG	HQBPGG	HQHLGG
$q\bar{q}$	HQHOQA	HQHDQA ASHDQA CTHDQA	HQBDQA	HQHPQA ASHPQA CTHPQA	HQBPQA	HQHLQA
qg		CTHDQG		HQHPQG ASHPQG CTHPQA	HQBPQG	HQHLQG

Table 8: Fortran routines for the various subprocesses.

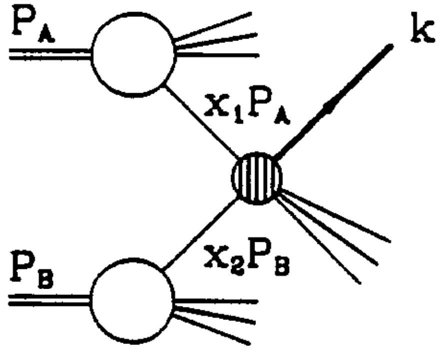

Fig. 1

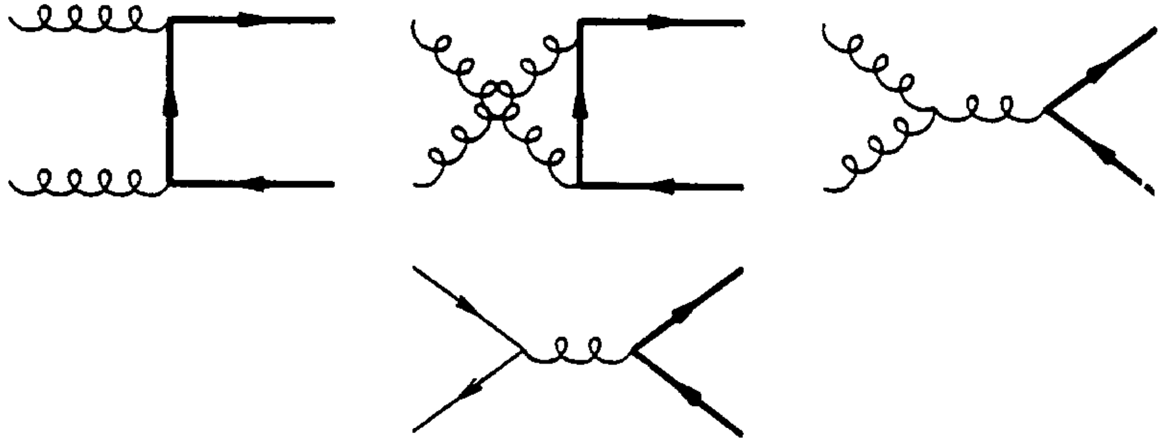

Fig. 2

a) b)

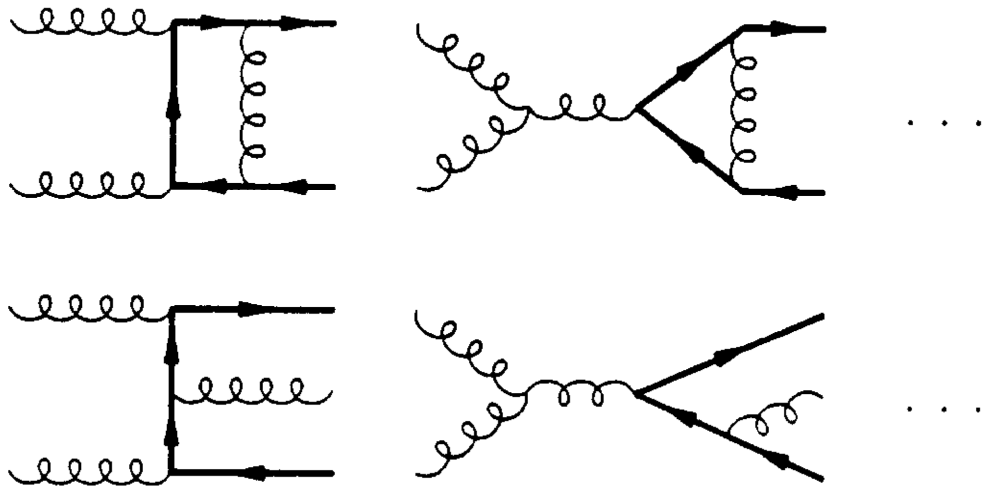

Fig. 3

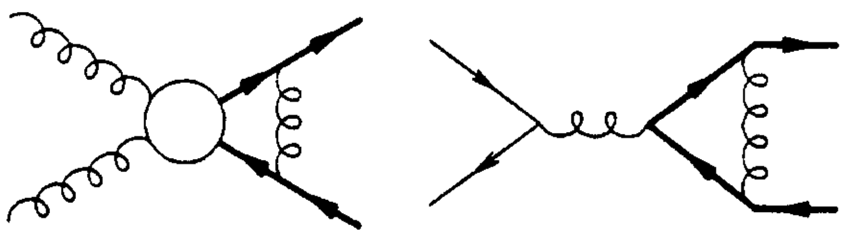

a) b)

Fig. 4

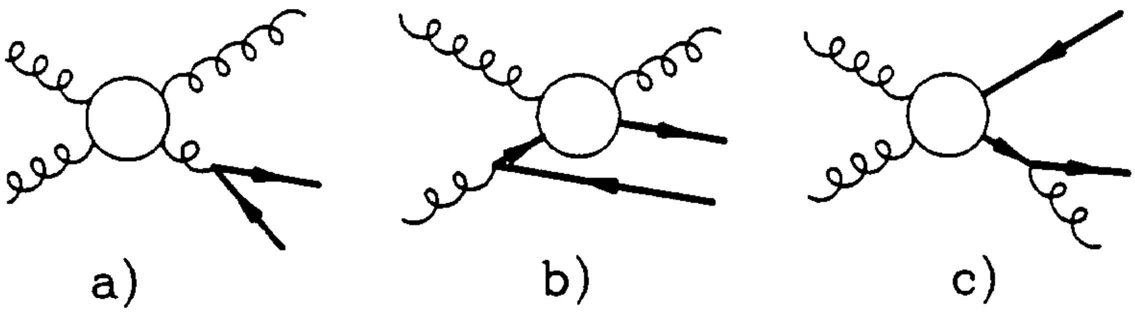

Fig. 5

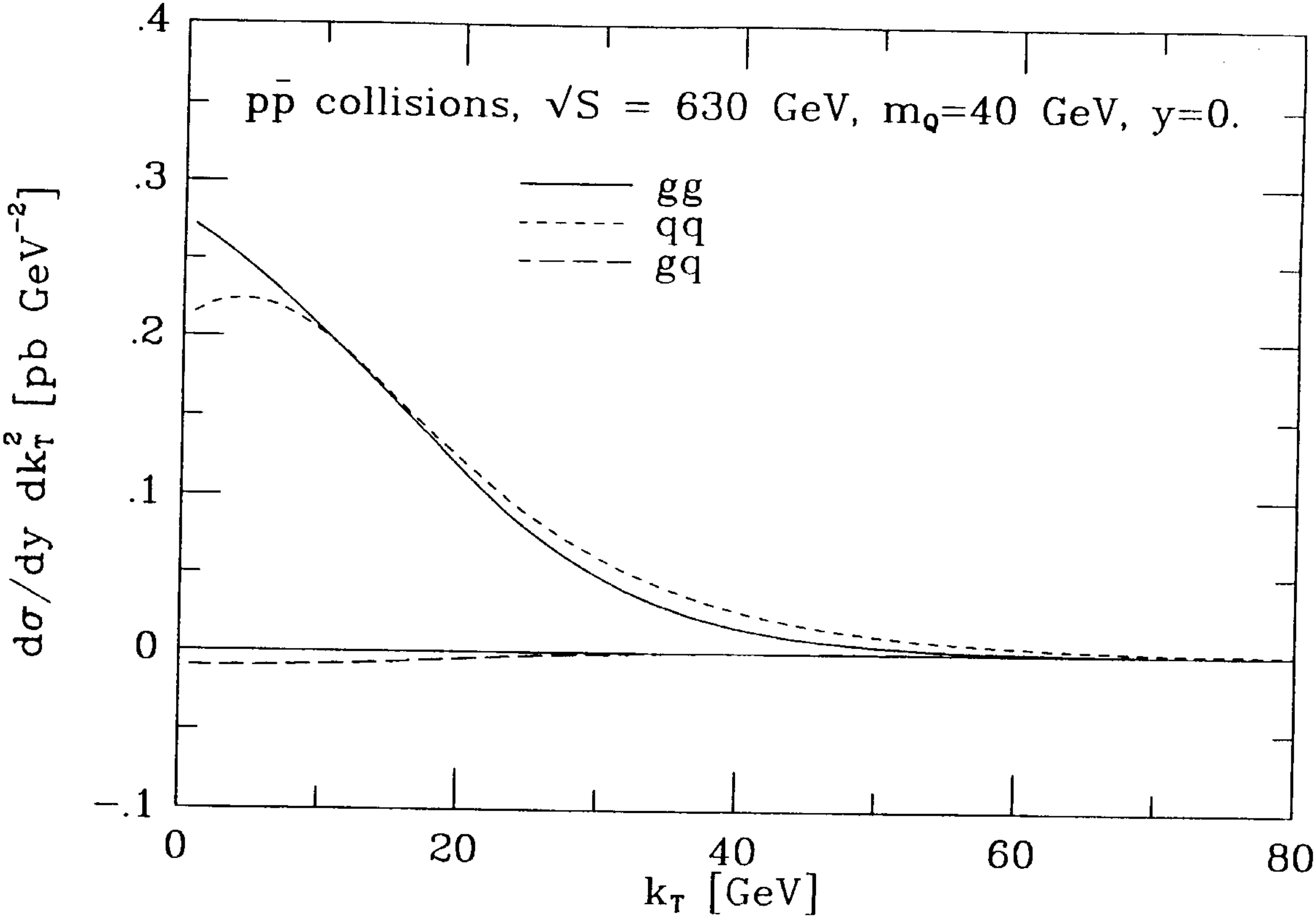

$p\bar{p}$ collisions, $\sqrt{S}$ = 630 GeV, m_Q=40 GeV, y=0.
gg
qq
gq
$d\sigma/dy\ dk_T^2$ [pb GeV^{-2}]
.4
.3
.2
.1
0
−.1
0
20
40
60
80
k_T [GeV]

Fig. 6

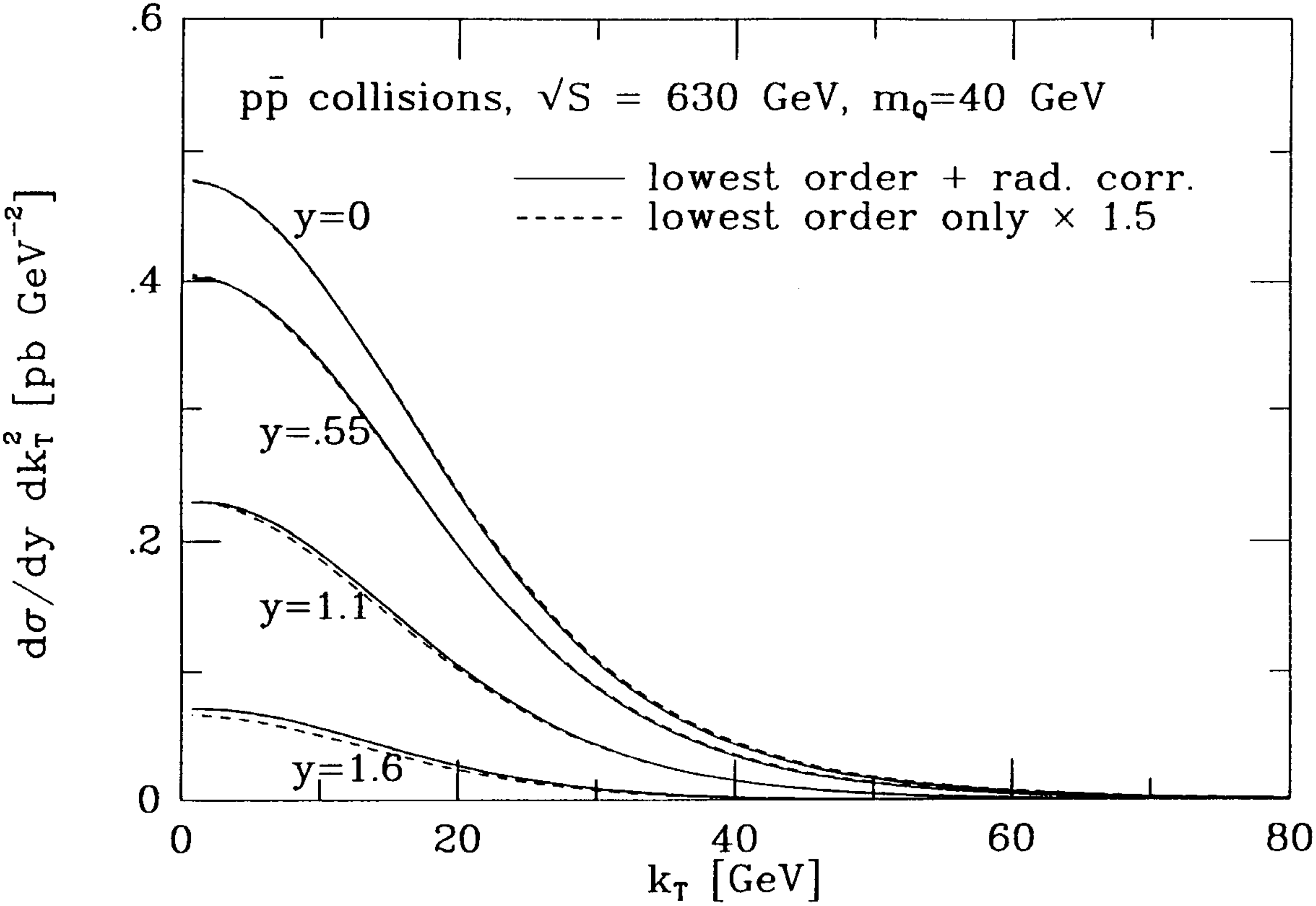
pp̄ collisions, √S = 630 GeV, m_Q=40 GeV
lowest order + rad. corr.
lowest order only × 1.5
y=0
y=.55
y=1.1
y=1.6
dσ/dy dk_T^2 [pb GeV^-2]
k_T [GeV]
.6
.4
.2
0
0
20
40
60
80

Fig. 7

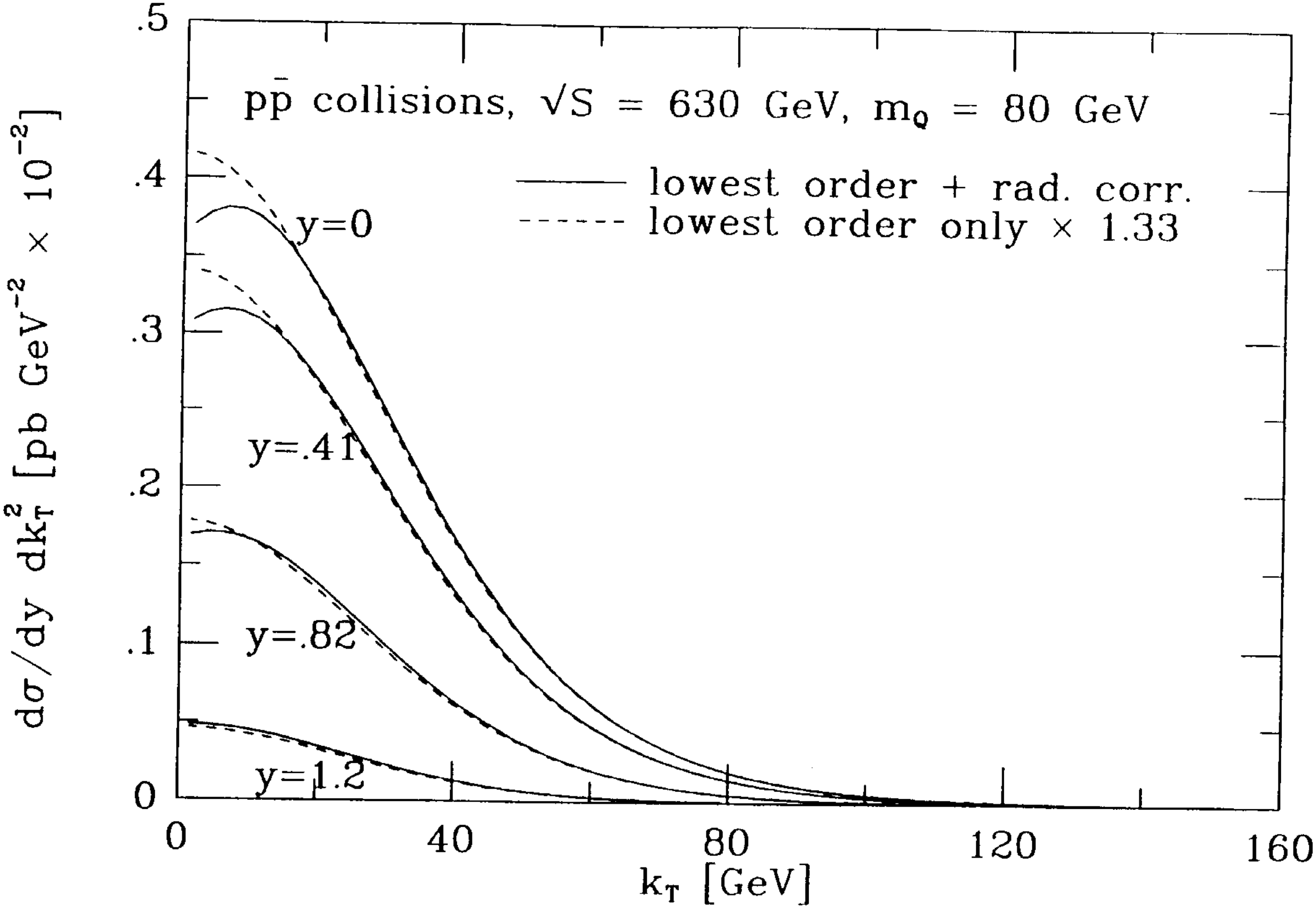

$p\bar{p}$ collisions, $\sqrt{S}$ = 630 GeV, m_Q = 80 GeV
lowest order + rad. corr.
lowest order only × 1.33
y=0
y=.41
y=.82
y=1.2
$d\sigma/dy\, dk_T^2$ [pb GeV^{-2} × 10^{-2}]
k_T [GeV]
0
.1
.2
.3
.4
.5
0
40
80
120
160

Fig. 8

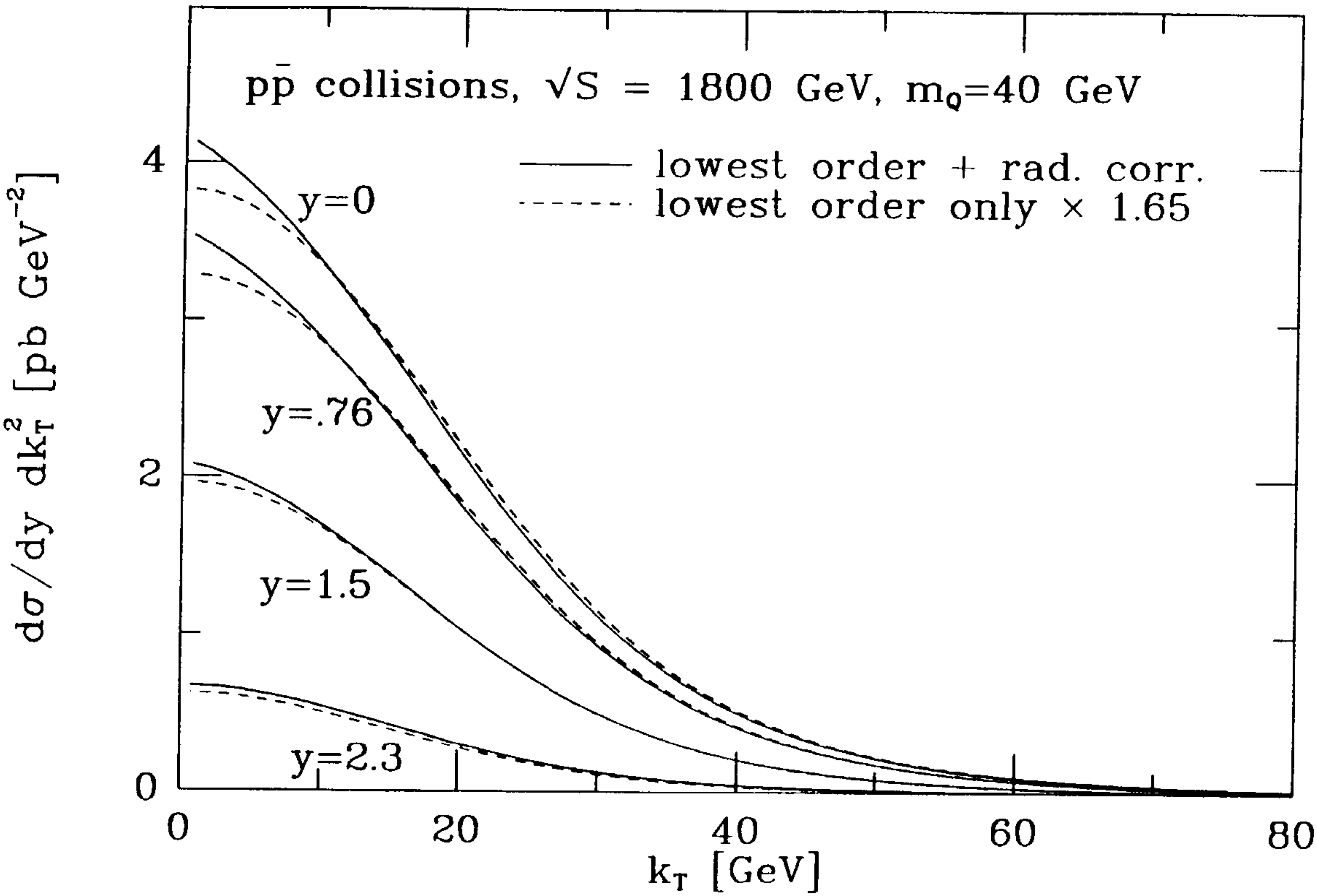

$p\bar{p}$ collisions, $\sqrt{S}$ = 1800 GeV, m_Q=40 GeV
lowest order + rad. corr.
lowest order only × 1.65
y=0
y=.76
y=1.5
y=2.3
$d\sigma/dy\ dk_T^2$ [pb GeV^{-2}]
4
2
0
0
20
40
60
80
k_T [GeV]

Fig. 9

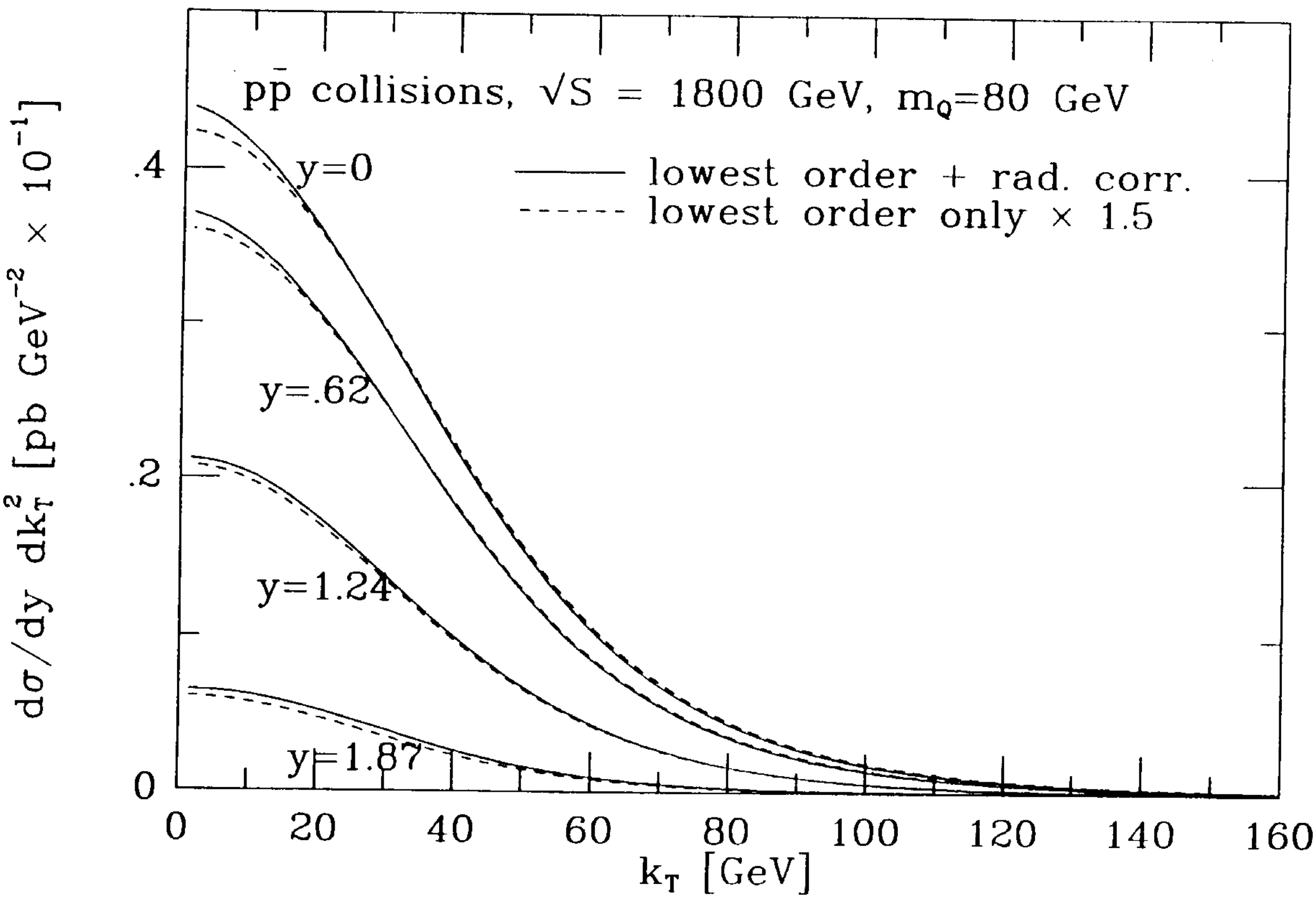
$p\bar{p}$ collisions, $\sqrt{S}$ = 1800 GeV, m_Q=80 GeV
lowest order + rad. corr.
lowest order only × 1.5
y=0
y=.62
y=1.24
y=1.87
$d\sigma/dy\ dk_T^2$ [pb GeV^{-2} × 10^{-1}]
k_T [GeV]
0
.2
.4
0
20
40
60
80
100
120
140
160

Fig. 10

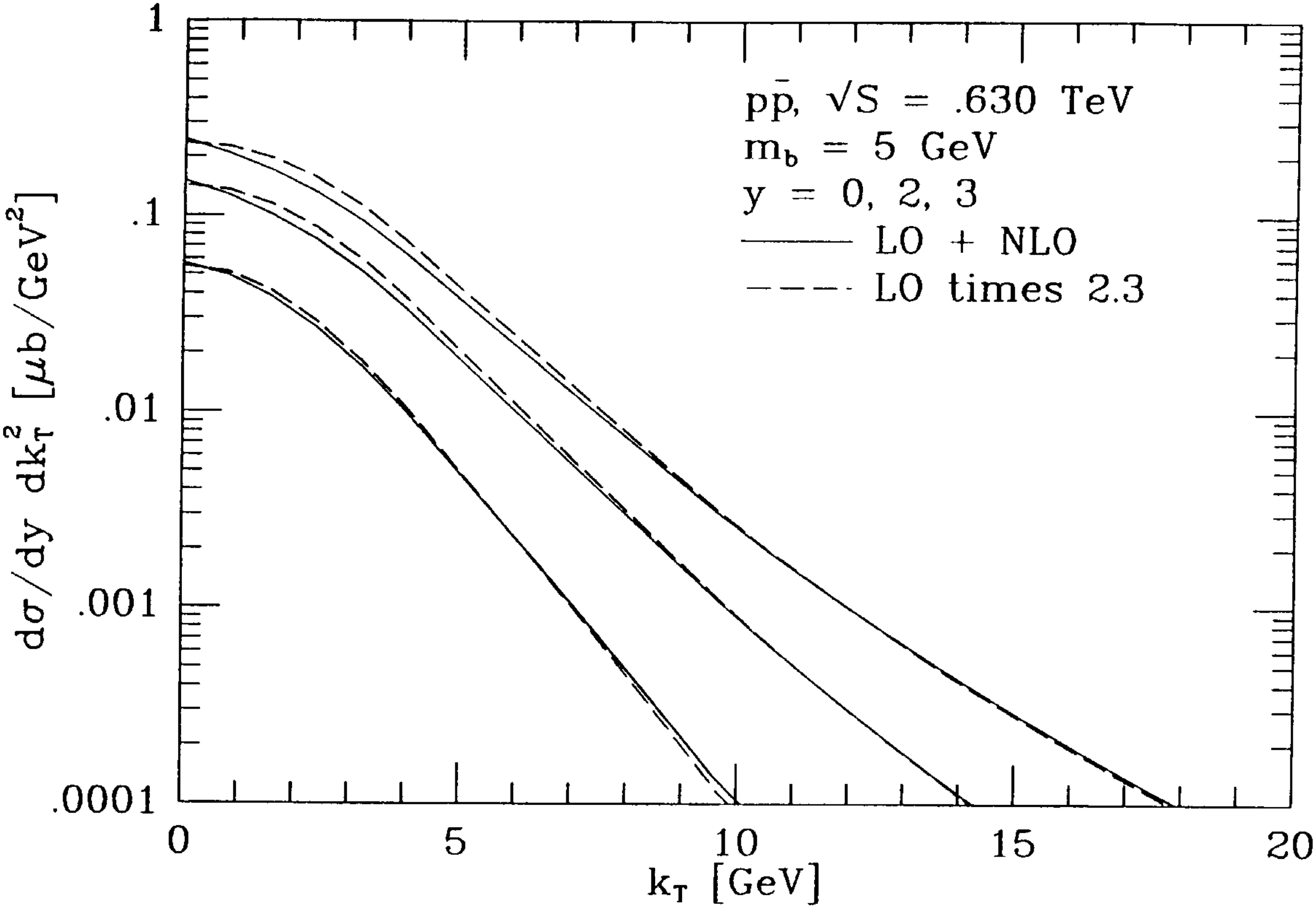

$p\bar{p}$, $\sqrt{S}$ = .630 TeV
m_b = 5 GeV
y = 0, 2, 3
LO + NLO
LO times 2.3
1
.1
.01
.001
.0001
0
5
10
15
20
k_T [GeV]
$d\sigma/dy\ dk_T^2$ [μb/GeV^2]

Fig. 11

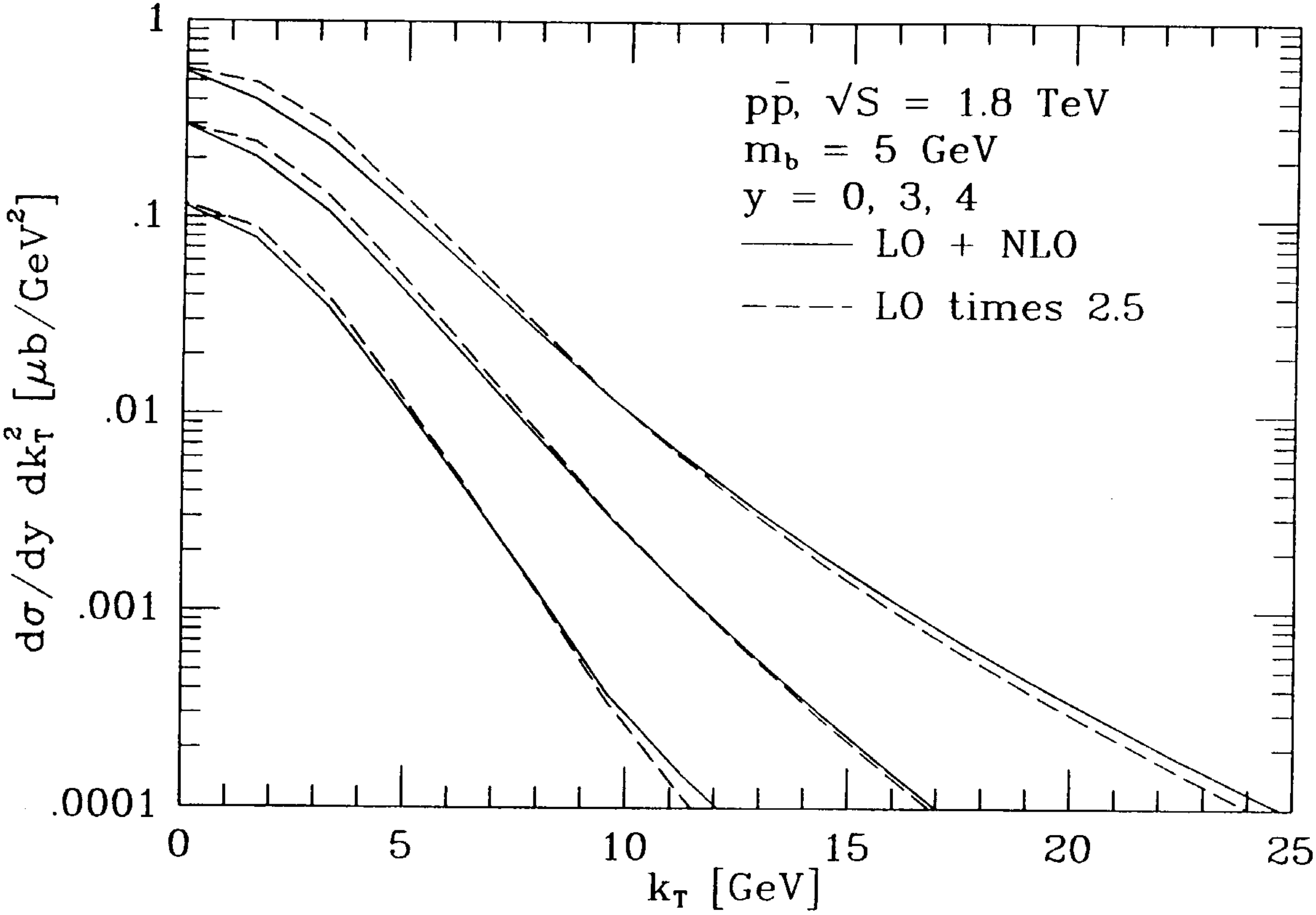

pp̄, √S = 1.8 TeV
m_b = 5 GeV
y = 0, 3, 4
LO + NLO
LO times 2.5
1
.1
.01
.001
.0001
dσ/dy dk_T^2 [μb/GeV^2]
0
5
10
15
20
25
k_T [GeV]

Fig. 12

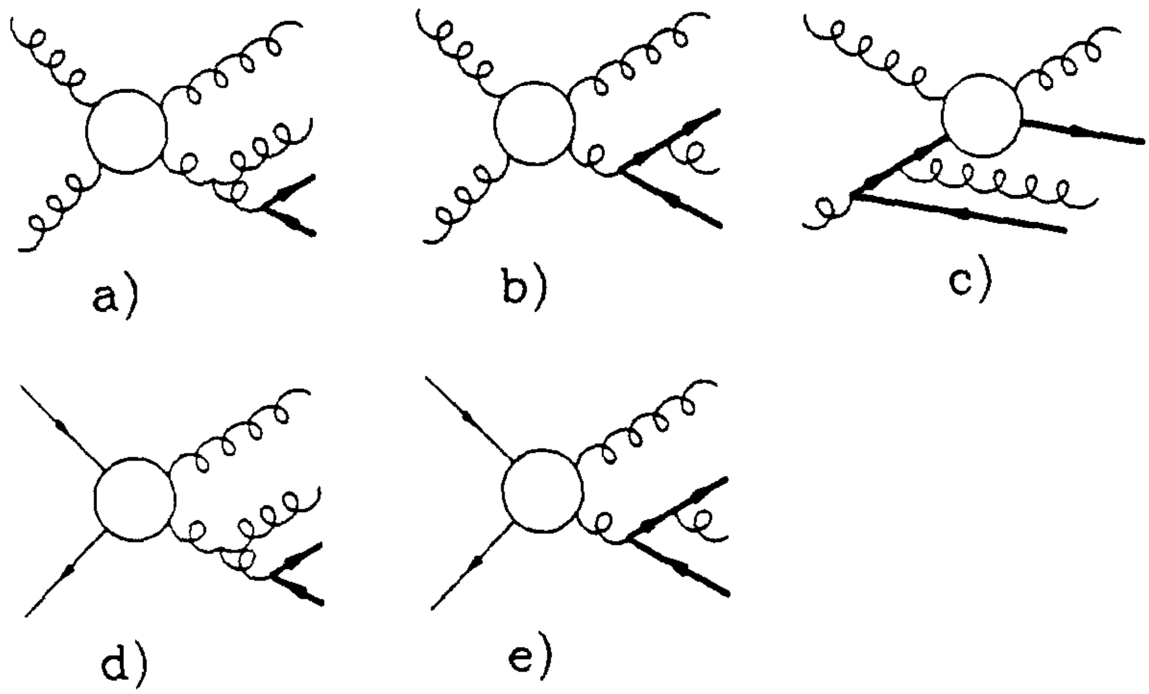

Fig. 13

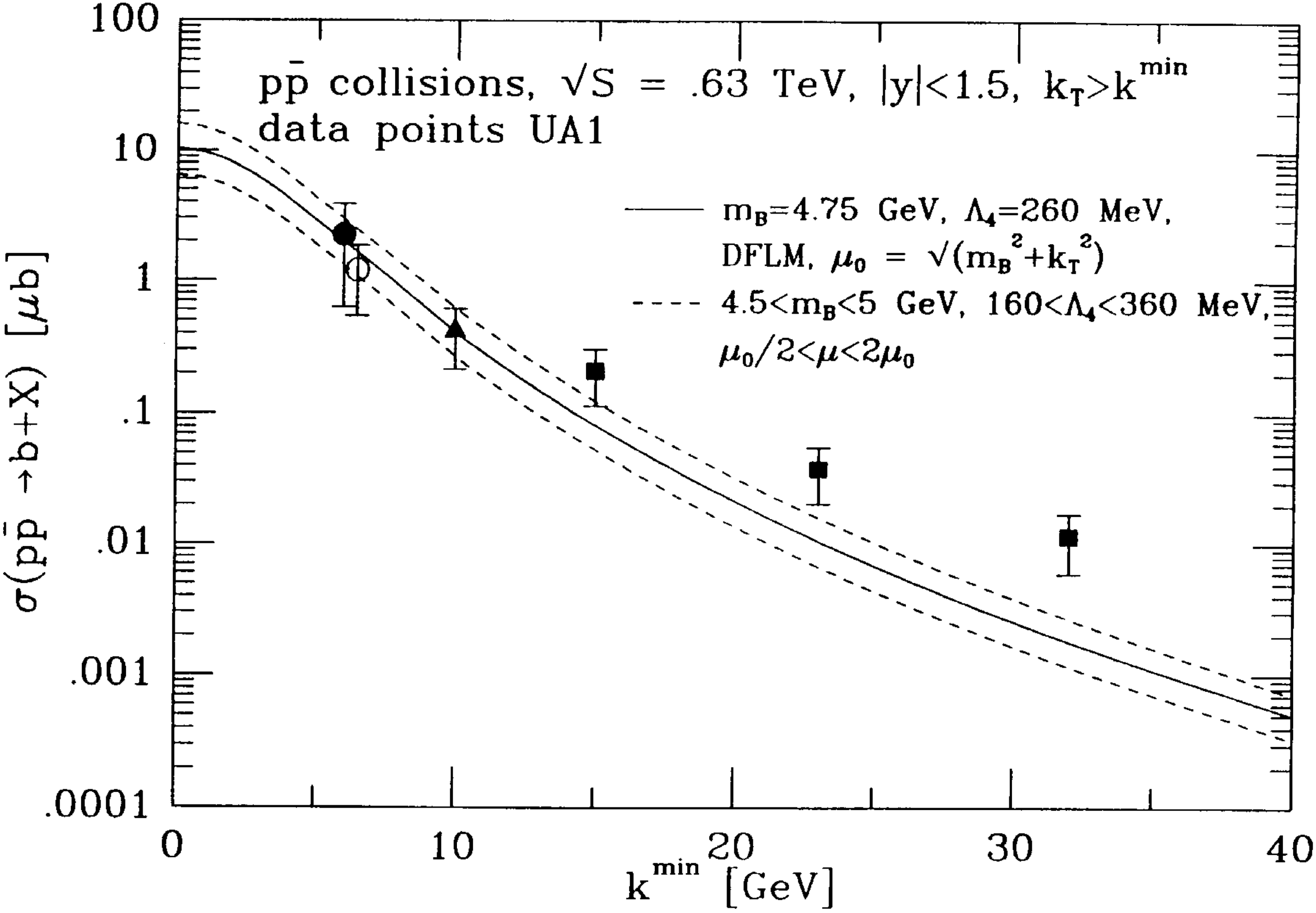

100
10
1
.1
.01
.001
.0001
0
10
20
30
40
$p\bar{p}$ collisions, $\sqrt{S}$ = .63 TeV, $|y|<1.5$, $k_T>k^{min}$
data points UA1
m_B=4.75 GeV, Λ_4=260 MeV,
DFLM, $\mu_0 = \sqrt{(m_B^2+k_T^2)}$
$4.5<m_B<5$ GeV, $160<\Lambda_4<360$ MeV,
$\mu_0/2<\mu<2\mu_0$
$\sigma(p\bar{p} \to b+X)$ [μb]
k^{min} [GeV]

Fig. 14

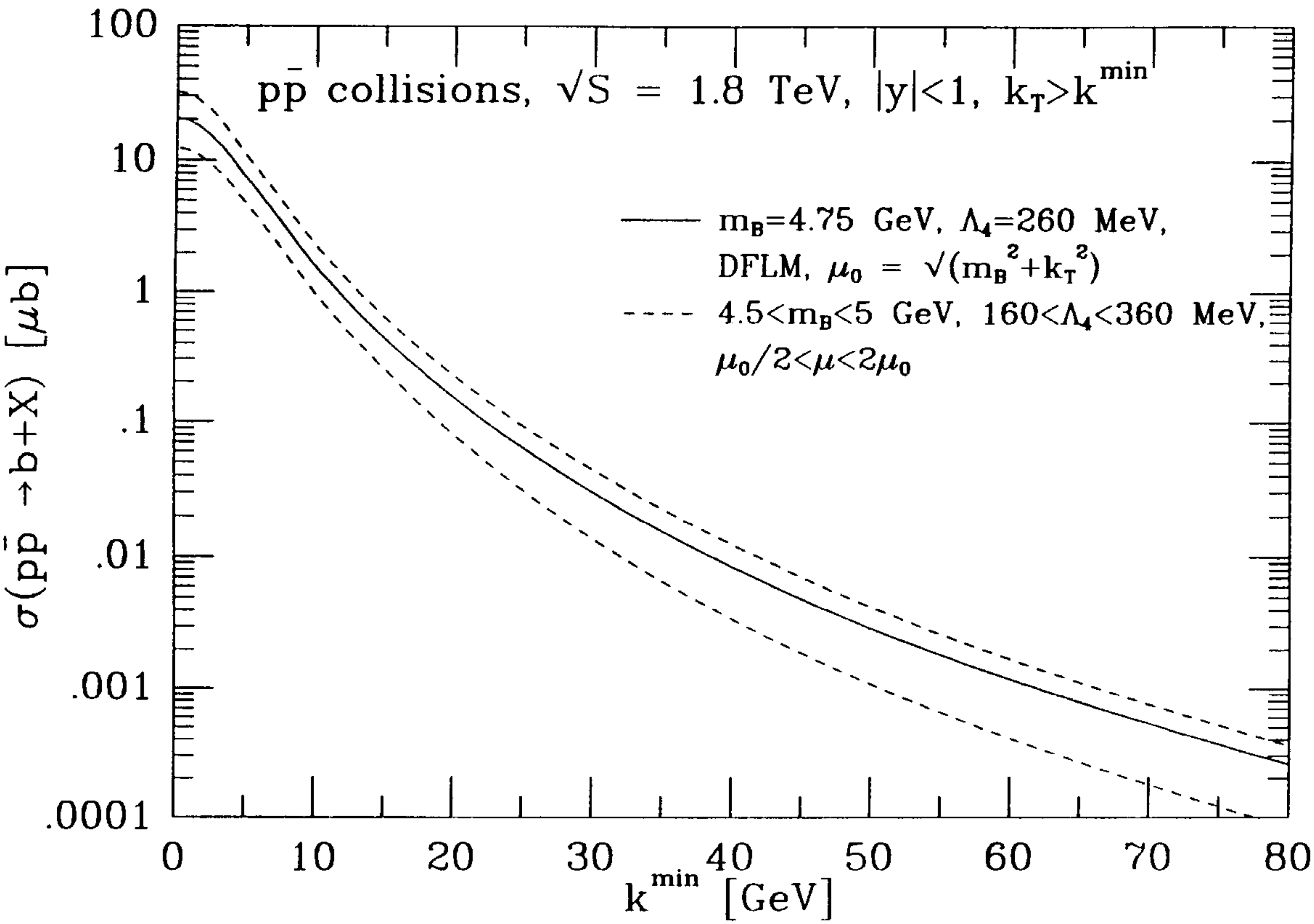

$p\bar{p}$ collisions, $\sqrt{S}$ = 1.8 TeV, $|y|<1$, $k_T>k^{min}$
m_B=4.75 GeV, Λ_4=260 MeV,
DFLM, $\mu_0 = \sqrt{(m_B^2+k_T^2)}$
4.5<m_B<5 GeV, 160<Λ_4<360 MeV,
$\mu_0/2<\mu<2\mu_0$
$\sigma(p\bar{p} \to b+X)$ [μb]
k^{min} [GeV]
100
10
1
.1
.01
.001
.0001
0
10
20
30
40
50
60
70
80

Fig. 15

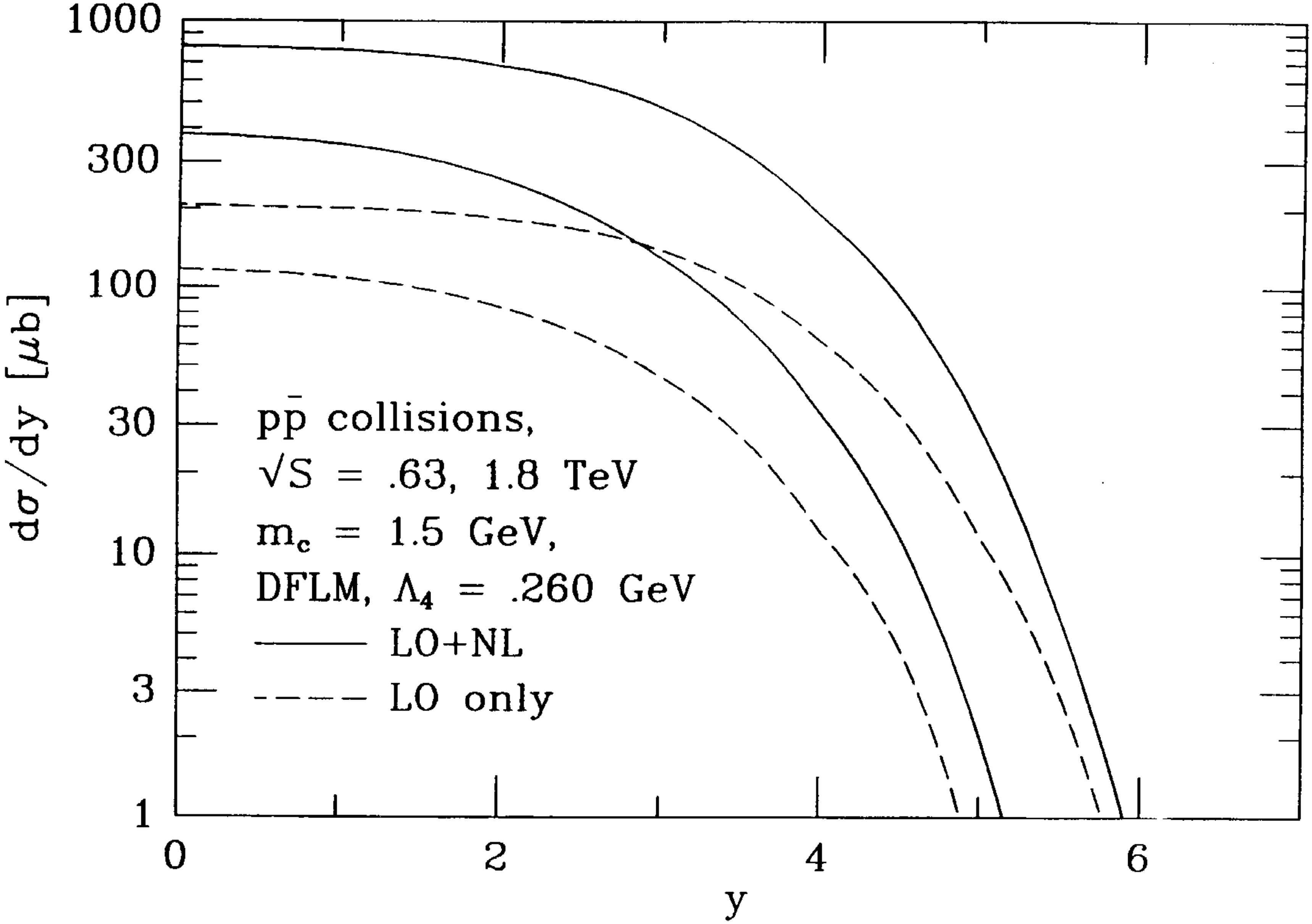
1000
300
100
30
10
3
1
dσ/dy [μb]
0
2
4
6
y
pp̄ collisions,
√S = .63, 1.8 TeV
m_c = 1.5 GeV,
DFLM, Λ_4 = .260 GeV
LO+NL
LO only

Fig. 16

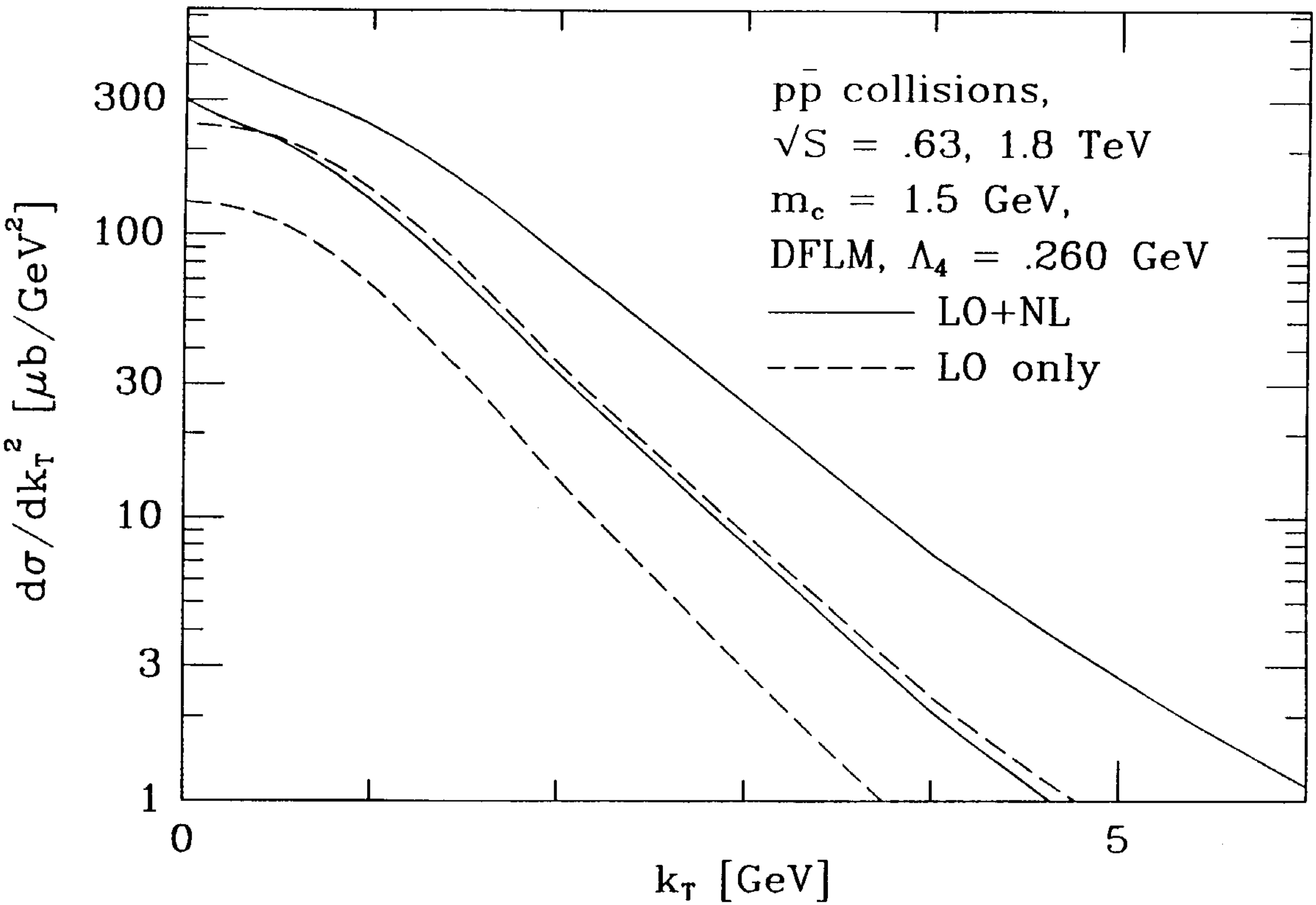
$p\bar{p}$ collisions,
$\sqrt{S}$ = .63, 1.8 TeV
m_c = 1.5 GeV,
DFLM, Λ_4 = .260 GeV
LO+NL
LO only
$d\sigma/dk_T^2$ [μb/GeV^2]
300
100
30
10
3
1
0
5
k_T [GeV]

Fig. 17

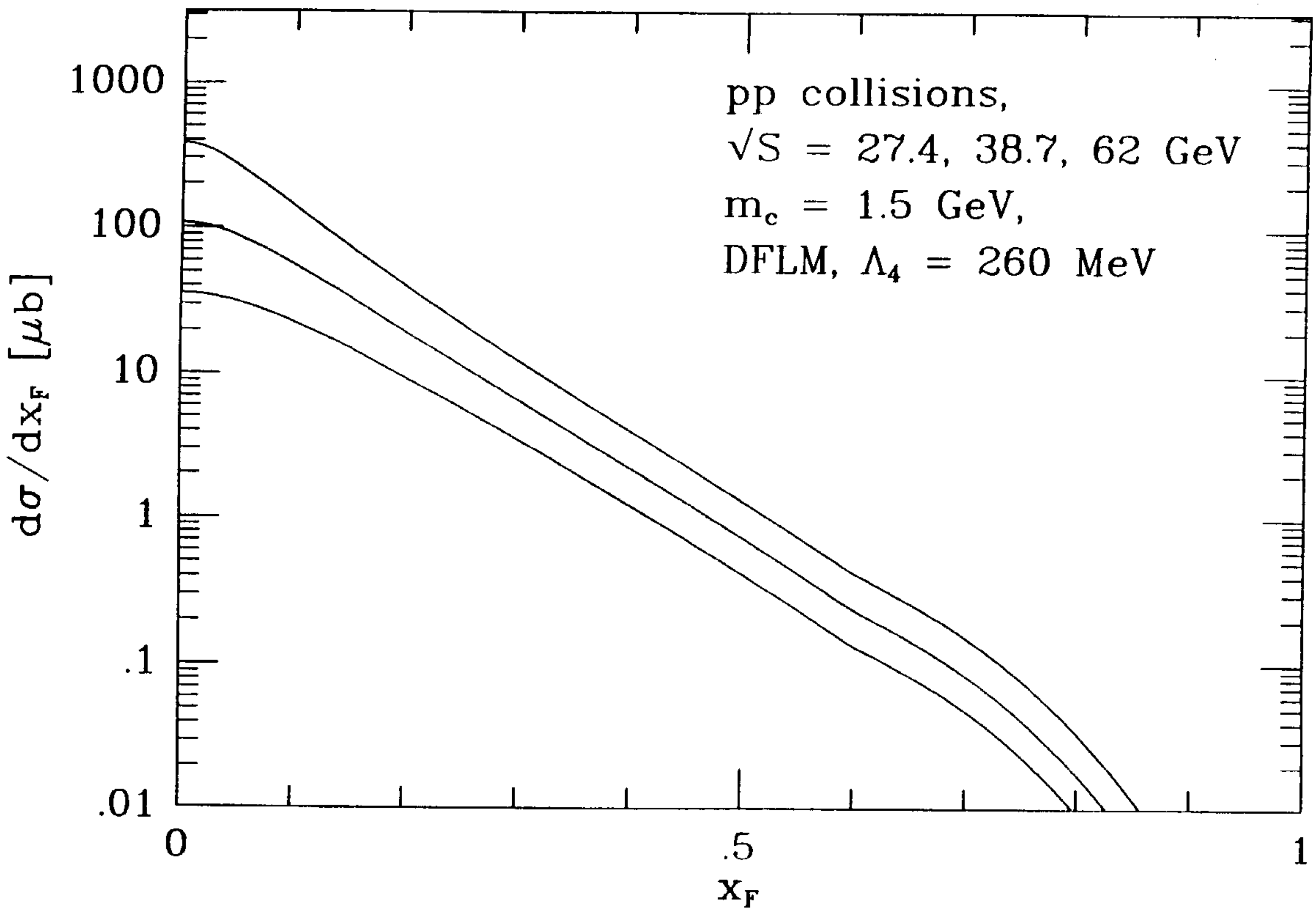
pp collisions,
√S = 27.4, 38.7, 62 GeV
m_c = 1.5 GeV,
DFLM, Λ_4 = 260 MeV
$d\sigma/dx_F$ [μb]
1000
100
10
1
.1
.01
0
.5
1
x_F

Fig. 18

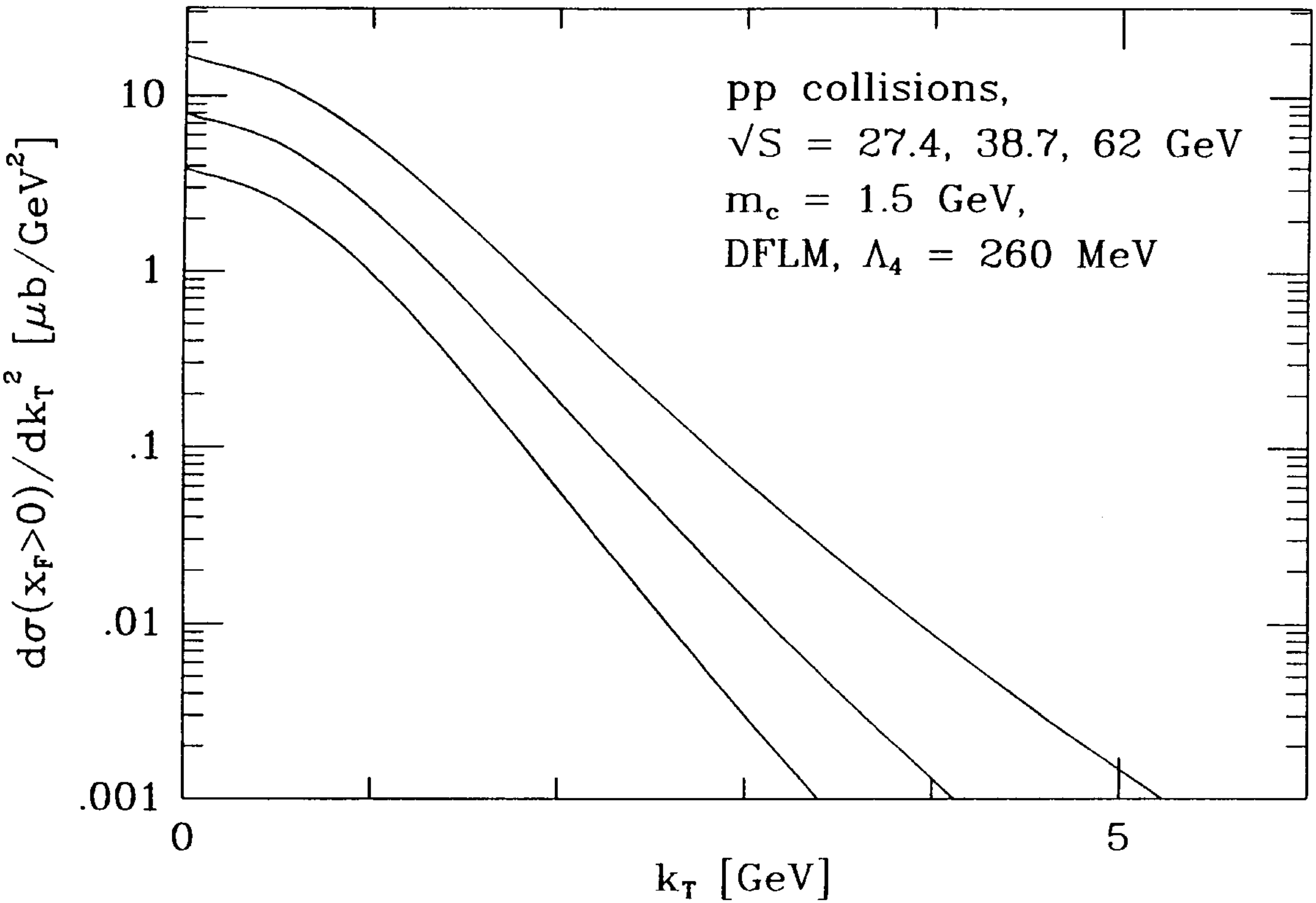

pp collisions,
$\sqrt{S}$ = 27.4, 38.7, 62 GeV
m_c = 1.5 GeV,
DFLM, Λ_4 = 260 MeV
10
1
.1
.01
.001
0
5
$d\sigma(x_F>0)/dk_T^2$ [μb/GeV^2]
k_T [GeV]

Fig. 19

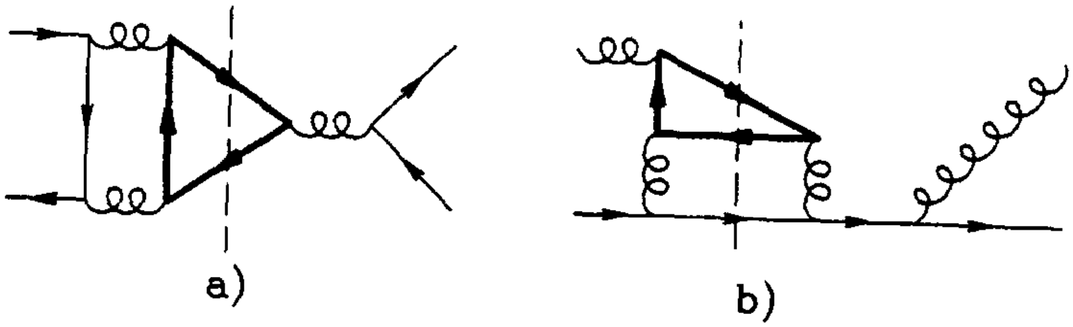

Fig. 20

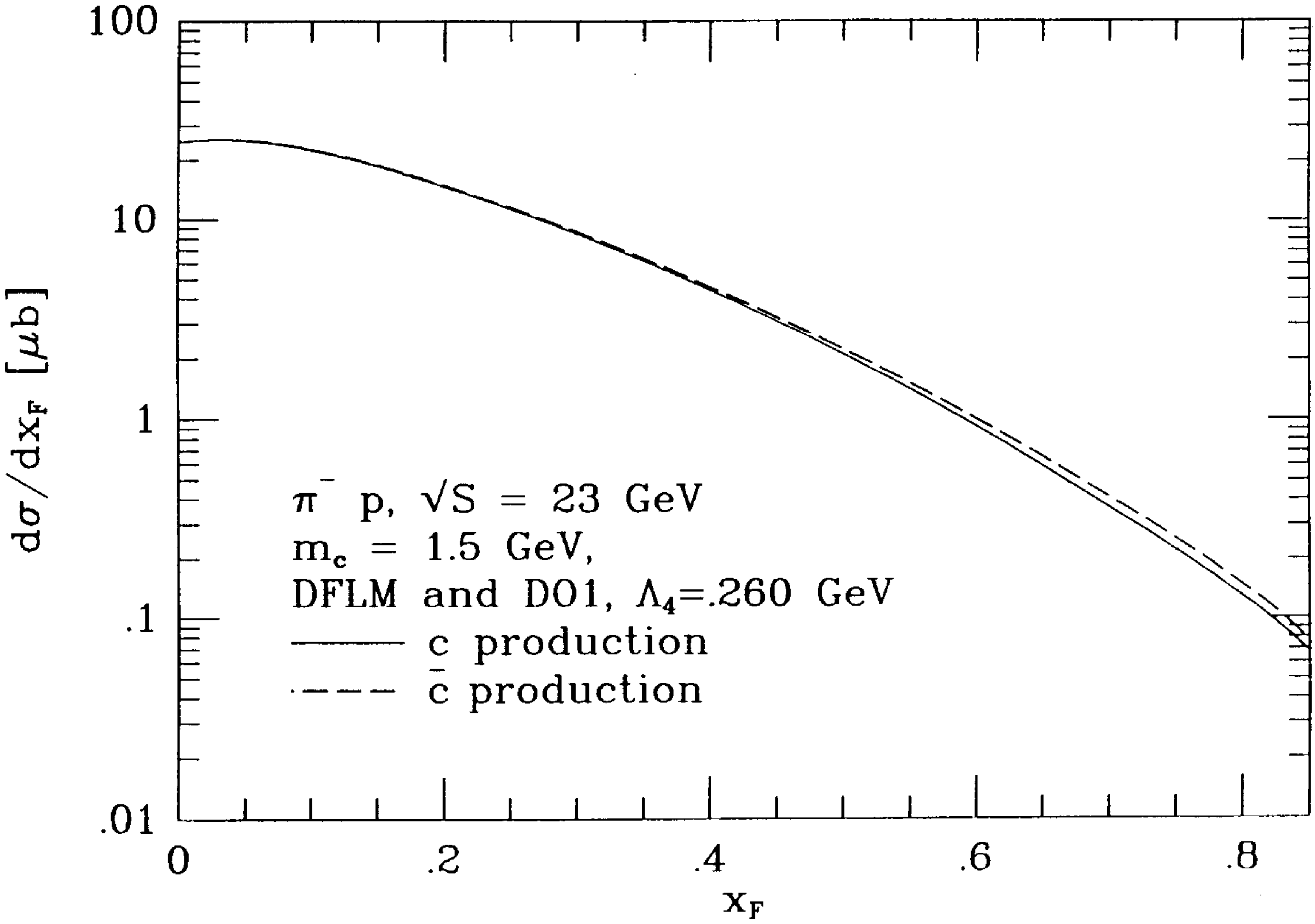
100
10
1
.1
.01
0
.2
.4
.6
.8
x_F
$d\sigma/dx_F$ [μb]
π^- p, $\sqrt{S}$ = 23 GeV
m_c = 1.5 GeV,
DFLM and DO1, Λ_4=.260 GeV
c production
$\bar{c}$ production

Fig. 21

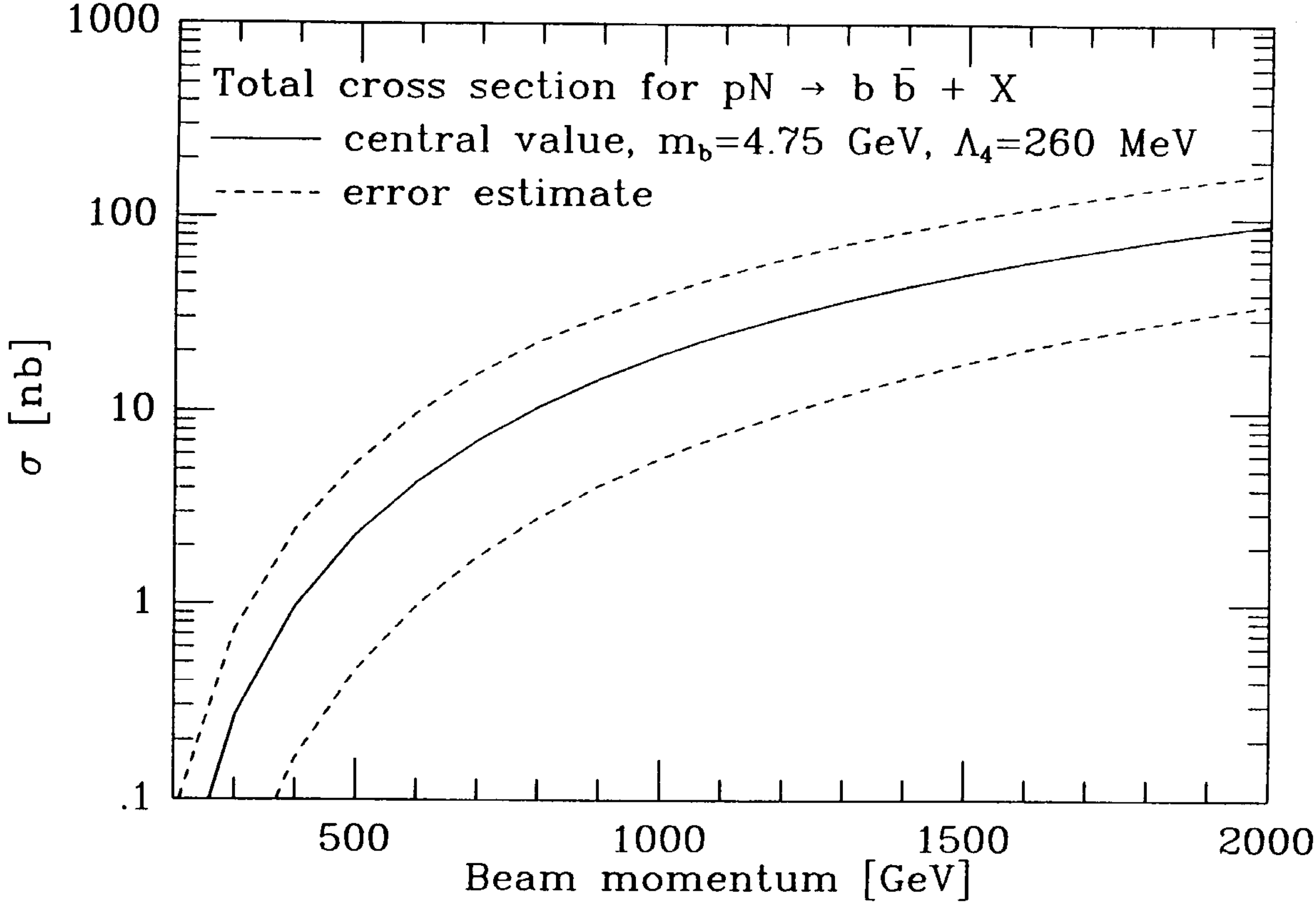

Total cross section for pN → b b̄ + X
central value, m_b=4.75 GeV, Λ_4=260 MeV
error estimate
1000
100
10
1
.1
σ [nb]
500
1000
1500
2000
Beam momentum [GeV]

Fig. 22

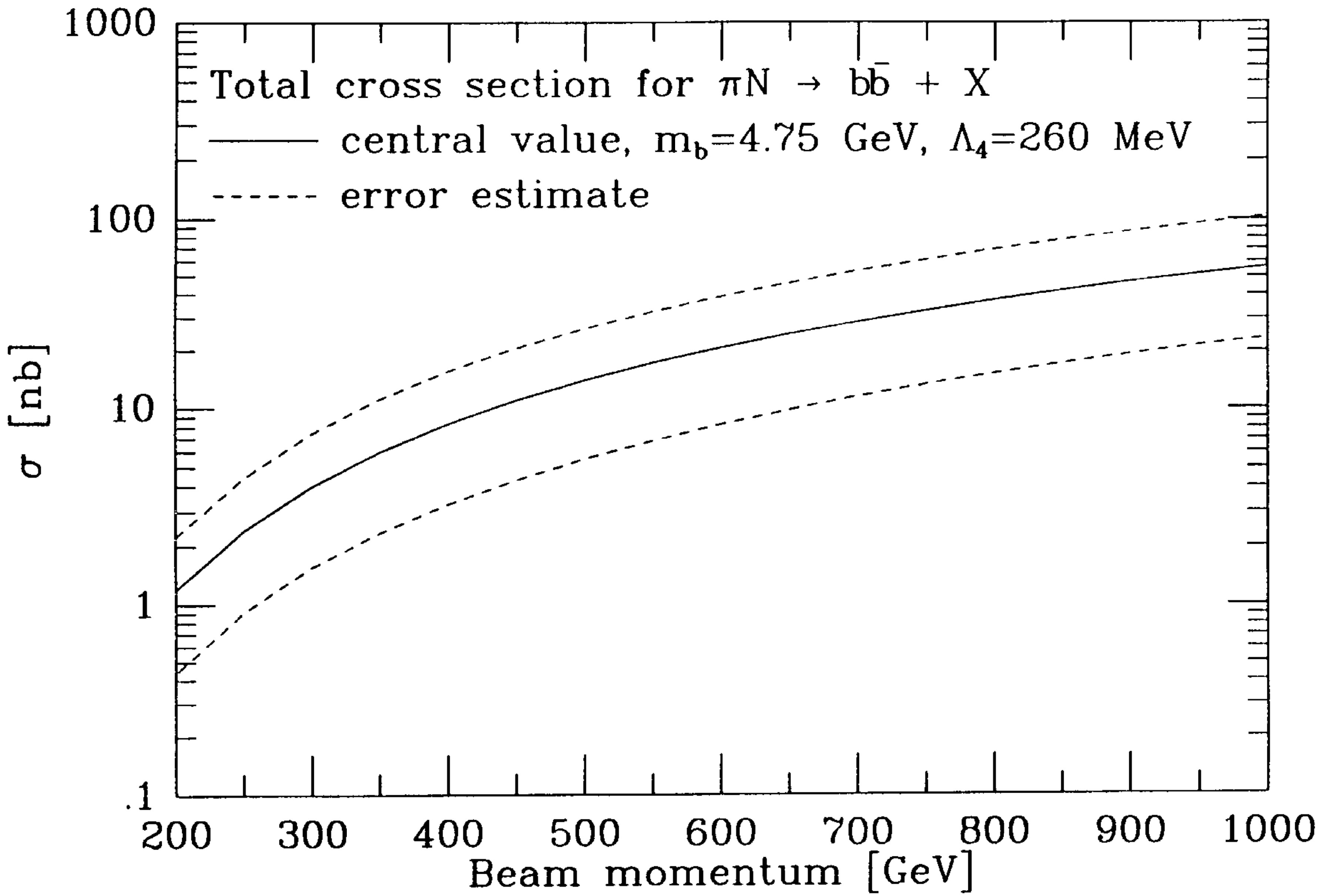

Total cross section for $\pi N \to b\bar{b} + X$
central value, m_b=4.75 GeV, Λ_4=260 MeV
error estimate
1000
100
10
1
.1
σ [nb]
200
300
400
500
600
700
800
900
1000
Beam momentum [GeV]

Fig. 23

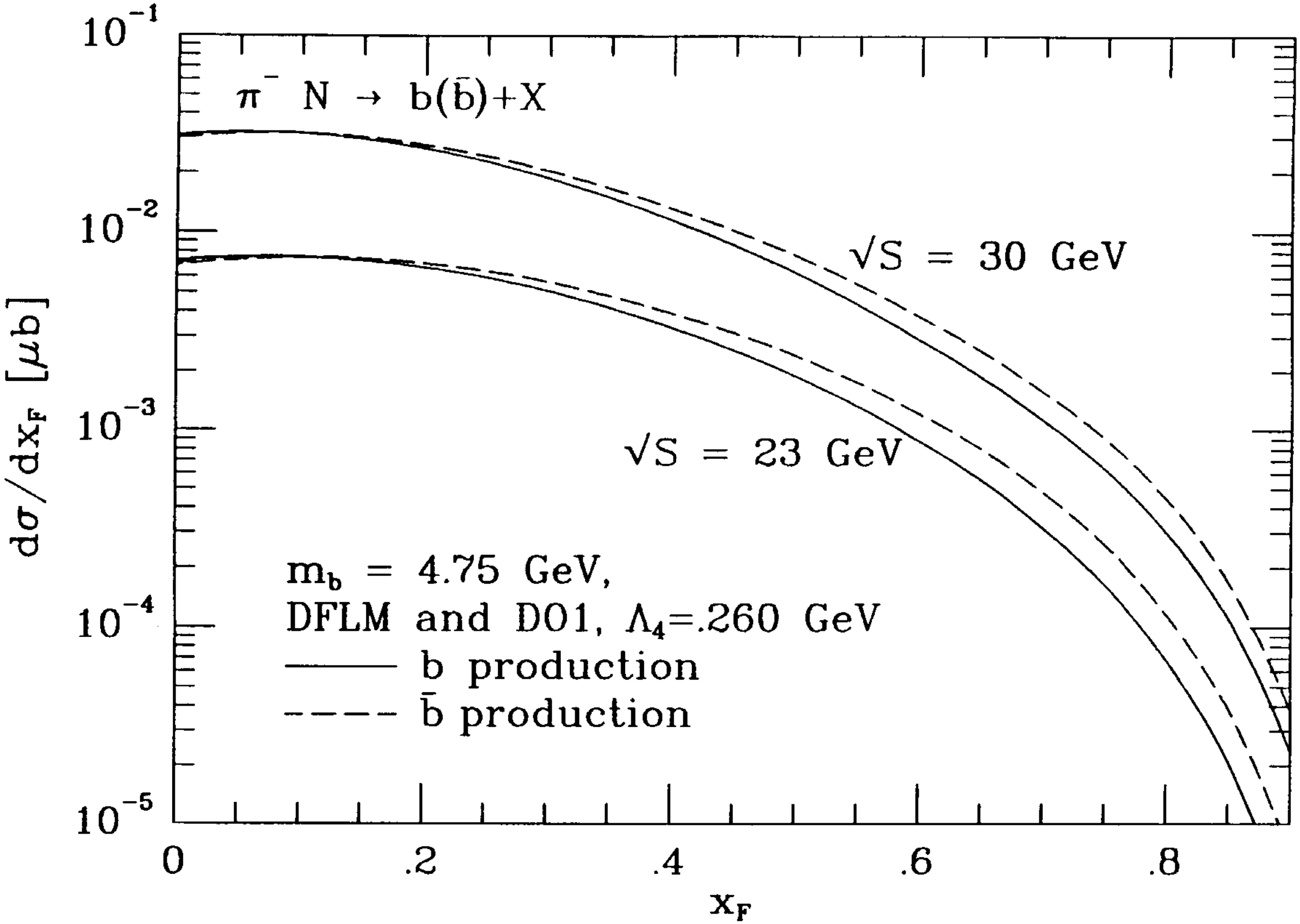
$\pi^- N \to b(\bar{b})+X$
$\sqrt{S}$ = 30 GeV
$\sqrt{S}$ = 23 GeV
m_b = 4.75 GeV,
DFLM and DO1, Λ_4=.260 GeV
b production
$\bar{b}$ production
$d\sigma/dx_F$ [μb]
x_F
10^{-1}
10^{-2}
10^{-3}
10^{-4}
10^{-5}
0
.2
.4
.6
.8

Fig. 24

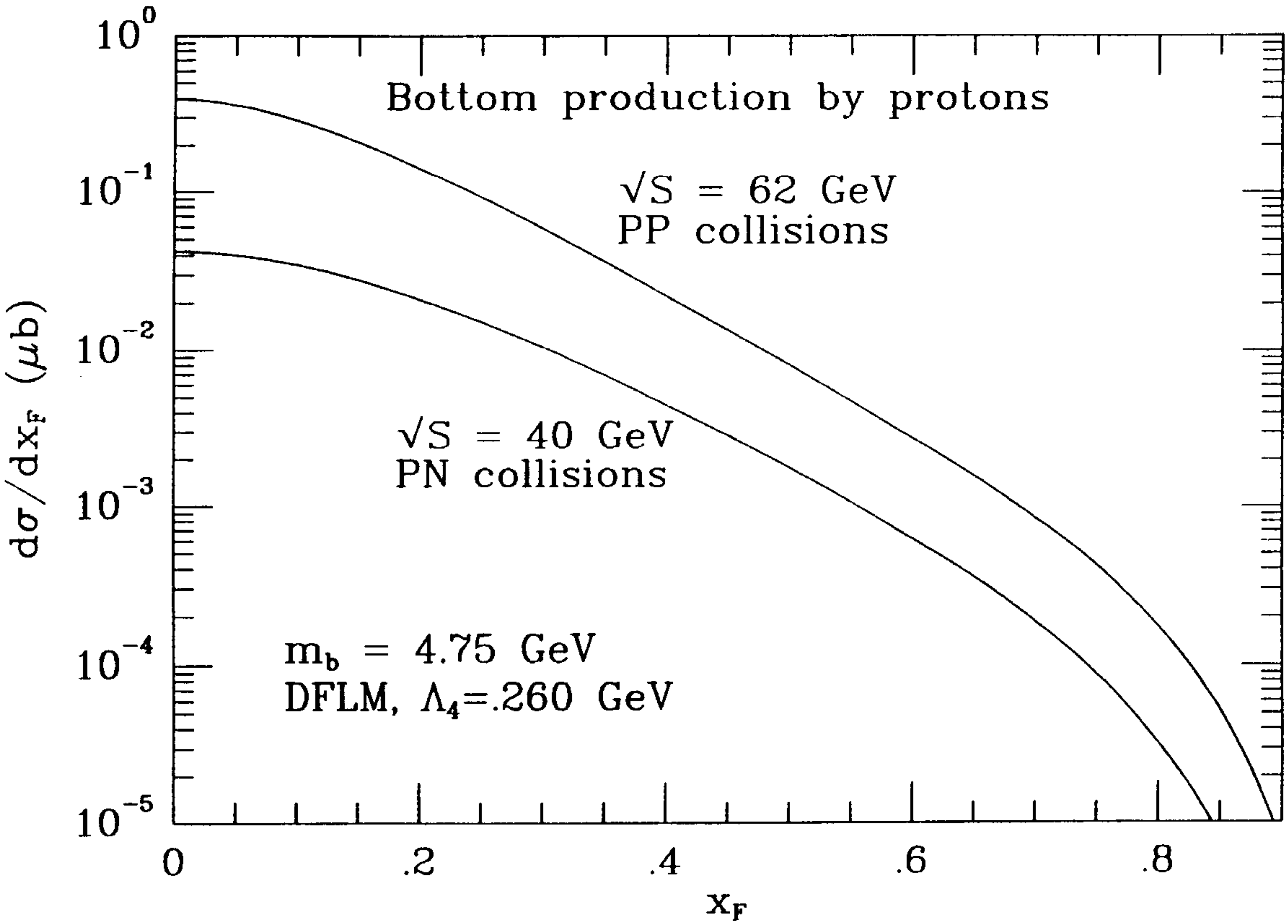

Bottom production by protons
√S = 62 GeV
PP collisions
√S = 40 GeV
PN collisions
m_b = 4.75 GeV
DFLM, Λ_4=.260 GeV
10^0
10^{-1}
10^{-2}
10^{-3}
10^{-4}
10^{-5}
$d\sigma/dx_F$ (μb)
0
.2
.4
.6
.8
x_F

Fig. 25

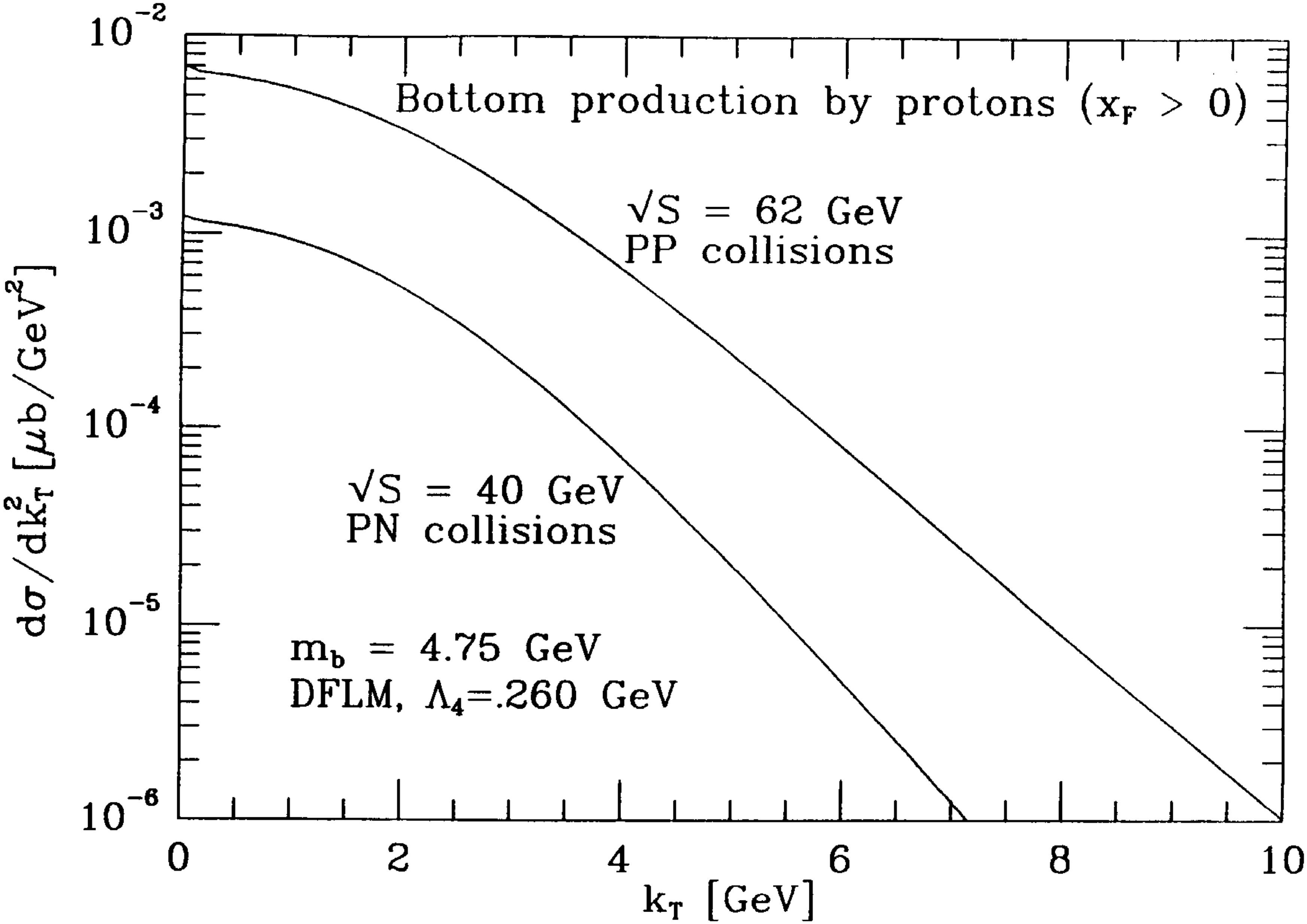
Bottom production by protons ($x_F > 0$)
$\sqrt{S}$ = 62 GeV
PP collisions
$\sqrt{S}$ = 40 GeV
PN collisions
m_b = 4.75 GeV
DFLM, Λ_4=.260 GeV
$d\sigma/dk_T^2$ [μb/GeV^2]
10^{-2}
10^{-3}
10^{-4}
10^{-5}
10^{-6}
0
2
4
6
8
10
k_T [GeV]

Fig. 26